

Theory of single photon detection by 'dirty' current-carrying superconducting strip based on the kinetic equation approach

D.Yu. Vodolazov

Institute for Physics of Microstructure, Russian Academy of Sciences, 603950, Nizhny Novgorod, GSP-105, Russia

(Dated: January 28, 2022)

Using kinetic equation approach we study dynamics of electrons and phonons in current-carrying superconducting nanostrips after absorption of single photon of near-infrared or optical range. We find that the larger the ratio $C_e/C_{ph}|_{T_c}$ (T_c is a critical temperature of superconductor, C_e and C_{ph} are specific heat capacities of electrons and phonons, respectively) the larger part of photon's energy goes to electrons, they become stronger heated and, hence, could thermalize faster during initial stage of hot spot formation. Thermalization time τ_{th} could be less than one picosecond for superconductors with $C_e/C_{ph}|_{T_c} \gg 1$ and small diffusion coefficient $D \simeq 0.5\text{cm}^2/\text{s}$ when thermalization occurs mainly due to electron-phonon and phonon-electron scattering in relatively small volume $\sim \xi^2 d$ (ξ is a superconducting coherence length, $d < \xi$ is a thickness of the strip). At larger times because of diffusion of hot electrons effective temperature inside the hot spot decreases, the size of hot spot increases, superconducting state becomes unstable and normal domain spreads in the strip at current larger than so-called detection current. We find dependence of detection current on the photon's energy, place of its absorption in the strip, width of the strip, magnetic field and compare it with existing experiments. Our results demonstrate that materials with $C_e/C_{ph}|_{T_c} \ll 1$ are bad candidates for single photon detectors due to small transfer of photon's energy to electronic system and large τ_{th} . We also predict that even several microns wide dirty superconducting bridge is able to detect single near-infrared or optical photon if its critical current exceeds 70 % of depairing current and $C_e/C_{ph}|_{T_c} \gtrsim 1$.

PACS numbers: 74.25.F-, 74.40.Gh

I. INTRODUCTION

Main idea of single photon detection by the current carrying superconducting strip is relatively simple. The absorbed photon heats the electrons in the restricted area of the strip (it is called as a hot spot), superconductivity is locally destroyed and critical current I_c of the strip is reduced up to $I_c^{spot} < I_c$. If transport current exceeds I_c^{spot} transition to the resistive state occurs and it is detected in the experiment.

At the present time there are several phenomenological models which offer different scenarios for appearance of the resistive response after photon absorption and which explain some experimental results [1–6] (see also recent review of models in Ref. [7]). The drawback of these models is that they use phenomenological assumptions about size of the hot region, level of suppression of superconductivity and part of the photon's energy which is stored in the electronic system. Besides, some of these models [1, 4, 6] operate with the number of nonequilibrium quasiparticles in order to find the suppression of magnitude of superconducting order parameter $|\Delta|$. One should have in mind, that this approach is quantitatively valid only when the deviation of quasiparticle (electron) distribution function $n(\epsilon)$ from equilibrium occurs in the narrow energy interval $\delta\epsilon$ near the superconducting gap $\epsilon_g \gg \delta\epsilon$ which is not true in the case of the hot spot formation in thin superconducting strip, especially at its initial stage, when the effective temperature of electrons could be larger than the bath temperature in several times. Therefore one can expect only qualitative validity

of the approaches using ideas of Rothwarf-Taylor model [8].

Below we formulate two problems which we solve to understand what material could be the good candidate for usage in superconducting nanowire single photon detector. First problem concerns the question what part of the energy of the photon goes to the electronic system and how it is related with material parameters of the superconducting strip. The second problem is connected with the question how fast the electrons (throughout the paper by electrons we mean quasiparticle excitations) are thermalized and what is the role of electron-electron inelastic scattering. It is known, that all materials which show good ability to detect single photons are extremely dirty superconducting strips with small diffusion coefficient $D \simeq 0.5\text{cm}^2/\text{s}$ and low critical temperature $T_c \lesssim 10K$. First of all, small D does not allow fast diffusion of electrons which favors their fast thermalization, because the energy of absorbed photon is confined in relatively small volume at initial stage of hot spot formation leading to relatively high 'temperature' of hot electrons. Secondly, the smaller D the smaller is the electron-electron inelastic relaxation time τ_{e-e} which also decreases thermalization time τ_{th} and increases the capability to detect single photon. Indeed, if thermalization time τ_{th} of electrons is larger than their diffusion time $\tau_{D,w} \simeq w^2/4D$ across the strip with width w the photon's energy will be smeared over the large area which leads to smaller influence on superconducting properties and it complicates photon's detection.

To answer above questions we numerically solve kinetic equations for electron and phonon distribution functions,

taking into account electron-phonon, phonon-electron and electron-electron scattering. First of all we study the initial stage of the electron-phonon downconversion cascade on time scale comparable with the characteristic time of variation of $|\Delta| - \tau_\Delta \simeq \hbar/|\Delta| \simeq \hbar/k_B T_c$ during which one cannot expect strong suppression of superconducting order parameter and electrons diffuse only on distance $\sim \sqrt{D\tau_{|\Delta|}}$ which is about of superconducting coherence length in dirty superconductors $\xi \sim \sqrt{\hbar D/|\Delta|}$. We find that electron-phonon downconversion cascade and thermalization in electronic system depends not only on strength of electron-electron scattering, but also on ratio of electronic C_e and phonon C_{ph} heat capacities taken at $T = T_c$. Indeed, the larger the ratio $C_e/C_{ph}|_{T_c}$ the larger part of phonon's energy goes to electronic system, its effective 'temperature' becomes higher and thermalization time τ_{th} is shorter. We show that relatively short $\tau_{th} \simeq \tau_{|\Delta|}$ could be reached in superconductors with large ratio $C_e/C_{ph}|_{T_c} \gg 1$ when thermalization occurs mainly via electron-phonon and phonon-electron scattering.

Dynamics of hot spot at times $t \gtrsim \tau_{|\Delta|}$ we study in two limits. In the limit of short thermalization time ($\tau_{th} \simeq \tau_{|\Delta|} \ll \tau_{D,w}$) we use two temperature model and solve heat conductance equations (taking into account the Joule dissipation) for electron and phonon temperatures coupled with modified Ginzburg-Landau equation for superconducting order parameter. In the limit of large thermalization time ($\tau_{th} \simeq \tau_{D,w}$) we assume uniform distribution of electron and phonon effective temperatures across the strip by time $t \simeq \tau_{D,w}$. In both limits we find the current-energy relation, dependence of the cut-off photon's energy on the temperature at fixed ratio $I/I_{dep}(T)$ (I_{dep} is a depairing current), study the role of the magnetic field and how current-energy relation depends on the strip's width. We show, that rel-

atively narrow (with width about 100-200 nm) superconducting strip with small ratio $C_e/C_{ph}|_{T_c} \ll 1$ needs current close to I_{dep} to be able to detect single photon with energy about 1 eV. On contrary, such a strip with ratio $C_e/C_{ph}|_{T_c} \gtrsim 1$ can detect the same photon at the current much smaller than depairing current. And, finally, we predict that even wide superconducting strip with $C_e/C_{ph}|_{T_c} \gtrsim 1$ and width of about several microns can detect single infrared or optical photon if the strip can be biased, without a loss of superconductivity, at $I \gtrsim 0.7I_{dep}(T)$.

The structure of the paper is following. In Sec. II we present basic equations. In Sec. III we show results on the initial stage of hot spot formation (on time scale about of $\tau_{|\Delta|}$ after photon's absorption) when its radius is smaller than the coherence length. In Sec. IV we study the case when instability of superconducting state occurs at the moment when the hot electrons reach both edges of the strip and form hot belt (limit of large τ_{th}), while in Sec. V we consider the opposite case when superconducting state becomes unstable before the hot spot expands across the strip (limit of small τ_{th}). In Sec. VI we compare our results with existing theories and experiments. In Sec. VII we formulate our main results.

II. EQUATIONS

In this section we present equations which we use to study the dynamics of electron and phonon distribution functions in superconducting strip at the initial stage of hot spot formation after absorption of the single photon. First of all these are the kinetic equations for electron n_ϵ and phonon N_ϵ distribution functions

$$N_1 \frac{\partial n}{\partial t} = D \nabla ((N_1^2 - R_2^2) \nabla n) - R_2 \frac{\partial n}{\partial \epsilon} \frac{\partial |\Delta|}{\partial t} + I_{e-ph}(n, N) + I_{e-e}(n), \quad (1)$$

$$\frac{\partial N}{\partial t} = -\frac{N - N_{eq}(T)}{\tau_{esc}} + I_{ph-e}(N, n), \quad (2)$$

where $I_{e-ph}(n, N)$, $I_{ph-e}(N, n)$ and $I_{e-e}(n)$ are the electron-phonon, phonon-electron and electron-electron collision integrals

$$\begin{aligned} I_{e-ph}(n, N) = & -\frac{1}{(k_B T_c)^3} \frac{1}{\tau_0} [\\ & \int_0^\epsilon d\epsilon_1 M(\epsilon, \epsilon_1) (\epsilon - \epsilon_1)^2 ([1 + 2N_{\epsilon-\epsilon_1}] (n_\epsilon - n_{\epsilon_1}) + n_\epsilon (1 - 2n_{\epsilon_1}) + n_{\epsilon_1}) + \\ & \int_\epsilon^{\epsilon + \hbar\omega_D} d\epsilon_1 M(\epsilon, \epsilon_1) (\epsilon - \epsilon_1)^2 ([1 + 2N_{\epsilon_1-\epsilon}] (n_\epsilon - n_{\epsilon_1}) - n_\epsilon (1 - 2n_{\epsilon_1}) - n_{\epsilon_1}) + \\ & \int_0^{\hbar\omega_D - \epsilon} d\epsilon_1 M(\epsilon, -\epsilon_1) (\epsilon + \epsilon_1)^2 ([1 + 2N_{\epsilon_1+\epsilon}] (n_\epsilon + n_{\epsilon_1} - 1) - n_\epsilon (1 - 2n_{\epsilon_1}) - n_{\epsilon_1} + 1)], \end{aligned} \quad (3)$$

$$\begin{aligned}
I_{ph-e}(N, n) = & \frac{\gamma}{\tau_0 k_B T_c} \left[\int_0^\epsilon d\epsilon_1 M(\epsilon_1, -(\epsilon - \epsilon_1)) \times \right. \\
& \times (n_{\epsilon_1} n_{\epsilon-\epsilon_1} + N_\epsilon (n_{\epsilon-\epsilon_1} + n_{\epsilon_1} - 1)) + \\
& \left. + 2 \int_0^\infty d\epsilon_1 M(\epsilon_1, (\epsilon + \epsilon_1)) ((1 - n_{\epsilon_1}) n_{\epsilon+\epsilon_1} + N_\epsilon (n_{\epsilon+\epsilon_1} - n_{\epsilon_1})) \right], \quad (4)
\end{aligned}$$

$$M(\epsilon, \pm \epsilon_1) = N_1(\epsilon) N_1(\epsilon_1) \mp R_2(\epsilon) R_2(\epsilon_1),$$

$$\begin{aligned}
I_{e-e}(n) = & \frac{\alpha_{e-e}}{\tau_0 k_B T_c} \int_0^\infty \int_0^\infty d\epsilon_1 d\epsilon_2 [\\
& + \frac{E_1}{|\epsilon - \epsilon_1|} (n_\epsilon (1 - n_{\epsilon_1}) (1 - n_{\epsilon_2}) (1 - n_{\epsilon-\epsilon_1-\epsilon_2}) - (1 - n_\epsilon) n_{\epsilon_1} n_{\epsilon_2} n_{\epsilon-\epsilon_1-\epsilon_2}) H_v(\epsilon - \epsilon_1 - \epsilon_2) \\
& + E_2 \left(\frac{1}{|\epsilon + \epsilon_1|} + \frac{2}{|\epsilon - \epsilon_2|} \right) (n_\epsilon n_{\epsilon_1} (1 - n_{\epsilon_2}) (1 - n_{\epsilon+\epsilon_1-\epsilon_2}) - (1 - n_\epsilon) (1 - n_{\epsilon_1}) n_{\epsilon_2} n_{\epsilon+\epsilon_1-\epsilon_2}) H_v(\epsilon + \epsilon_1 - \epsilon_2) \\
& + E_3 \left(\frac{1}{|\epsilon - \epsilon_1|} + \frac{2}{|\epsilon + \epsilon_2|} \right) (n_\epsilon (1 - n_{\epsilon_1}) n_{\epsilon_2} n_{\epsilon_1-\epsilon_2-\epsilon} - (1 - n_\epsilon) n_{\epsilon_1} (1 - n_{\epsilon_2}) (1 - n_{\epsilon_1-\epsilon_2-\epsilon})) H_v(\epsilon_1 - \epsilon_2 - \epsilon)], \quad (5)
\end{aligned}$$

$$\begin{aligned}
E_1 = & a(N_1(\epsilon) N_1(\epsilon_1) N_1(\epsilon_2) N_1(\epsilon - \epsilon_1 - \epsilon_2) - R_2(\epsilon) R_2(\epsilon_1) R_2(\epsilon_2) R_2(\epsilon - \epsilon_1 - \epsilon_2)) \\
& + b(N_1(\epsilon) R_2(\epsilon_1) R_2(\epsilon_2) N_1(\epsilon - \epsilon_1 - \epsilon_2) - R_2(\epsilon) N_1(\epsilon_1) N_1(\epsilon_2) R_2(\epsilon - \epsilon_1 - \epsilon_2)).
\end{aligned}$$

Coefficients E_2 and E_3 are expressed via E_1 in the following way: $E_2 = E_1(\epsilon_1 \rightarrow -\epsilon_1)$, $E_3 = E_1(\epsilon \rightarrow -\epsilon, \epsilon_1 \rightarrow -\epsilon_1)$. a and b are coefficients of order of unity [9, 10] and $H_v(x)$ is a Heaviside function.

$I_{e-ph}(n, N)$ and $I_{ph-e}(N, n)$ are written above for case when one can neglect renormalization of electron-phonon coupling constant due to disorder [11, 12] and

$$\frac{1}{\tau_0} = g \left(\frac{k_B T_c}{\hbar \omega_D} \right)^2 \frac{k_B T_c}{\hbar}, \quad (6)$$

is the familiar characteristic time introduced in Ref. [11] (ω_D is a Debye frequency and g is an electron-phonon coupling constant). Coefficient

$$\gamma = \frac{4\hbar\omega_D N(0)}{9N_{ion}} \left(\frac{\hbar\omega_D}{k_B T_c} \right)^2 = \frac{8\pi^2}{5} \frac{C_e}{C_{ph}} \Big|_{T=T_c}, \quad (7)$$

staying in front of I_{ph-e} collision integral is proportional to the ratio of the electronic $C_e(T) = (2\pi^2/3)k_B^2 N(0)T$ and phonon $C_{ph}(T) = (12\pi^4/5)N_{ion}k_B(k_B T/\hbar\omega_D)^3$ specific heat capacities at $T = T_c$ ($N(0)$ is the one spin density of states of electrons in the normal state at the Fermi energy E_F , N_{ion} is the density of ions).

Electron-electron collision integral in form of Eq. (5) is written for dirty quasi-2D metallic superconducting film with renormalized electron-electron coupling constant due to impurities. Coefficient α_{e-e}

$$\alpha_{e-e} = \tau_0 \frac{k_B T_c}{4\hbar} \frac{R_\square}{R_Q}, \quad (8)$$

describes the strength of electron-electron inelastic scattering (R_\square is the sheet resistance and $R_Q = 2\pi\hbar/e^2 \simeq 25.8\text{ kOhm}$ is the quantum resistance). In pure superconducting metal coefficients $1/|\epsilon \pm \epsilon_{1,2}|$ are absent and Eq. (5) transfers (with $\alpha_{e-e} = \tau_0(k_B T_c)^2/(2\hbar E_F)$) to expression present in Refs. [9, 10]. In the normal state $E_1 = E_2 = E_3 = a$ and Eq. (5) coincides (with $\alpha_{e-e} = \tau_0 k_B T_c / (4\hbar k_{FL})$ and $a = 1$) with e-e collision integral for 2D dirty metal from Ref. [13]. For dirty quasi-2D metallic normal film from Eqs. (1,5) and $\epsilon \gg k_B T$ it follows familiar inelastic e-e scattering time $\tau_{e-e}(\epsilon) = 4\hbar R_Q / (\epsilon R_\square)$ (see Eq. (4.4) in [14]).

Because coefficients a and b are unknown for any metal we put $a = 1$ and $b = 0$. Choice of $b = 0$ is connected with different expressions for E_i behind b which are present in Refs. [9, 10]. If we choose expression for E_i from Ref. [10] (as we do in our work) finite $b > 0$ leads to increase of τ_{e-e} for electrons having energy close to $|\Delta|$.

Spectral functions $N_1(\epsilon)$, $R_2(\epsilon)$, entering Eqs. (1, 3-5), has to be found in the dirty limit from the Usadel equation

$$\hbar D \nabla^2 \Theta + \left(2i\epsilon - \frac{D}{\hbar} q_s^2 \cos \Theta \right) \sin \Theta + 2|\Delta| \cos \Theta = 0, \quad (9)$$

where $q_s = mv_s = \hbar(\nabla\phi - 2eA/\hbar c)$ is the superfluid momentum, ϕ is a phase of superconducting order parameter $\Delta = |\Delta| e^{i\phi}$, $\cos \Theta = N_1(\epsilon) + iR_1(\epsilon)$ and $\sin \Theta = N_2(\epsilon) + iR_2(\epsilon)$. $N_1(\epsilon)N(0)$ has a meaning of density of

states of electrons in the superconducting state, while R_2 enters the equation for the superconducting order parameter.

A static self-consistency equation for the magnitude of the order parameter has a following form

$$\frac{1}{\lambda_{BCS}} = \int_0^{\hbar\omega_D} \frac{R_2}{|\Delta|} (1 - 2n_\epsilon) d\epsilon = \int_0^{\hbar\omega_D} \frac{R_2}{|\Delta|} (1 - 2n_\epsilon^{eq}) d\epsilon - \Phi_{neq}, \quad (10)$$

where $n_\epsilon^{eq} = 1/(\exp(\epsilon/k_B T) + 1)$ is an equilibrium distribution function of electrons (quasiparticles) and λ_{BCS} is a coupling constant in BCS theory. Suppression of $|\Delta|$ due to hot electrons is described by Φ_{neq}

$$\Phi_{neq} = 2 \int_0^{\hbar\omega_D} \frac{R_2}{|\Delta|} (n_\epsilon - n_\epsilon^{eq}) d\epsilon. \quad (11)$$

Very often, to describe suppression of the order parameter due to $n_\epsilon \neq n_\epsilon^{eq}$ the coordinate-dependent density of nonequilibrium electrons is used, which is determined as

$$N_{neq}(\vec{r})/V = 4N(0) \int_0^\infty N_1(n_\epsilon(\vec{r}) - n_\epsilon^{eq}) d\epsilon = 4N(0) \int_{|\Delta|}^\infty \frac{\epsilon(n_\epsilon(\vec{r}) - n_\epsilon^{eq})}{\sqrt{\epsilon^2 - |\Delta|^2}} d\epsilon. \quad (12)$$

The last expression is valid when one can neglect the gradient term and term with q_s^2 in Usadel equation which leads to

$$N_1(\epsilon) = \frac{\epsilon}{\sqrt{\epsilon^2 - |\Delta|^2}} H_v(\epsilon - |\Delta|), \quad (13)$$

and

$$R_2(\epsilon) = \frac{|\Delta|}{\sqrt{\epsilon^2 - |\Delta|^2}} H_v(\epsilon - |\Delta|). \quad (14)$$

Potential Φ_{neq} could be expressed via N_{neq}/V when deviation from equilibrium occurs in narrow energy interval near $|\Delta|$ and one can replace $\epsilon \simeq |\Delta|$ in numerator of Eq. (12) and take it off the integrand

$$\Phi_{neq}(\vec{r}) = 2 \int_{|\Delta|}^{\hbar\omega_D} \frac{n(\epsilon, \vec{r}) - n_{eq}(\epsilon)}{\sqrt{\epsilon^2 - |\Delta|^2}} d\epsilon \simeq \frac{N_{neq}(\vec{r})}{2N(0)|\Delta|V}. \quad (15)$$

When the deviation from equilibrium occurs in wide energy interval and/or it occurs at energies $\epsilon \gg |\Delta|$ then $\Phi_{neq} \neq N_{neq}/2N(0)|\Delta|V$ due to presence of extra factor ϵ in numerator of Eq. (12). In this case usage of the approach with number of nonequilibrium electrons cannot pretend for quantitative description and may be used only for qualitative analysis.

III. INITIAL STAGE OF HOT SPOT FORMATION

When deviation n_ϵ from n_ϵ^{eq} occurs in the volume smaller than ξ^3 and on time scale shorter than variation time of $|\Delta|$ one cannot expect strong suppression of superconductivity. Therefore, as a first approximation, at times $t < \tau_{|\Delta|}$ we study dynamics of n_ϵ and N_ϵ after absorption of the photon with $|\Delta| = const$. To simplify further the problem we also assume that the energy of the photon is distributed instantly over the volume $V_{init} = \pi\xi^2d$ (where $d < \xi$ is a thickness of the strip). In reality it takes time $\sim \xi^2/D = \tau_{|\Delta|}$ and below we argue that such a simplification should not change the main result of this section.

With above assumptions we numerically solve Eqs. (1-5), where we omit gradient terms and consider the case of zero current $I = 0$ (finite I leads to smearing of spectral functions at $\epsilon \simeq |\Delta|$ and does not influence our main result). We use different initial conditions, which corresponds to different physical situations. Electronic bubble initial condition

$$n_\epsilon(t=0) = n_\epsilon^{eq} + \frac{\alpha e^{-(\epsilon-\epsilon_0)^2/\delta\epsilon^2}}{\sqrt{\pi}\delta\epsilon}, \quad N_\epsilon(t=0) = N_\epsilon^{eq}, \quad (16)$$

($N_\epsilon^{eq} = 1/(\exp(\epsilon/k_B T) - 1)$ is an equilibrium distribution function of phonons) corresponds to absorption of the photon and creation of initial hot electrons at energy $\epsilon \simeq \epsilon_0 \gg \delta\epsilon$.

Phonon bubble initial condition

$$n_\epsilon(t=0) = n_\epsilon^{eq}, \quad N_\epsilon(t=0) = N_\epsilon^{eq} + \frac{\beta e^{-(\epsilon-\epsilon_0)^2/\delta\epsilon^2}}{\sqrt{\pi}\delta\epsilon}, \quad (17)$$

models situation when, for example, the molecule hits the strip and excites phonons with energy $\epsilon \simeq \epsilon_0$. Instead of photon bubble one can use phonon plateau initial condition (when acoustic phonons of all available energies $0 \leq \epsilon \leq \hbar\omega_D$ are excited with equal probability) and results are practically undistinguishable from the phonon bubble initial condition (if one is interested in thermalization time and dynamics of energy contained in electronic and phonon systems).

Third initial condition corresponds to extreme case of very high e-e relaxation rate, which at all energies $\epsilon < E_{photon}$ exceeds e-ph relaxation rate and at $\epsilon \simeq k_B T$ is larger than $1/\tau_{|\Delta|}$. In this situation electrons are thermalized at times $t \ll \tau_{|\Delta|}$ and all energy of the photon is kept in electronic system at $t = 0$

$$n_\epsilon(t=0) = \frac{1}{e^{\epsilon/k_B T_e} + 1}, \quad N_\epsilon(t=0) = N_\epsilon^{eq}. \quad (18)$$

In all cases we choose parameters α , β and T_e in Eqs. (16-18) in a way to keep absorbed energy per unit of vol-

ume the same. For electron bubble condition we choose $\epsilon_0 \gg \hbar\omega_D$, while for phonon bubble condition $\epsilon_0 \simeq \hbar\omega_D$.

During calculations we check that the energy is conserved

$$E_{photon}/V_{init} = (E_{ph} + E_e)/V_{init} - (E_{ph} + E_e)^{eq}/V_{init}, \quad (19)$$

where E_{ph} is the energy of phonon system in the Debye model with quadratic density of states $\mathcal{D}(\epsilon) = 9\epsilon^2/\hbar\omega_D$ per ion

$$E_{ph}/V_{init} = \frac{1}{V_{init}} \frac{\mathcal{D}(\hbar\omega_D)}{\hbar(\hbar\omega_D)^2} \int_0^{\hbar\omega_D} \epsilon^3 N_\epsilon d\epsilon = \frac{E_0}{\gamma} \int_0^{\hbar\omega_D/k_B T_c} \tilde{\epsilon}^3 N_{\tilde{\epsilon}} d\tilde{\epsilon}, \quad (20)$$

E_e is the energy of electrons(quasiparticles) in the superconductor

$$\begin{aligned} E_e/V_{init} &= \\ 4N(0) \left(\int_0^\infty \epsilon N_1 n_\epsilon d\epsilon - \frac{|\Delta|^2}{4} \left(\frac{1}{2} + \ln \left(\frac{\Delta_0}{|\Delta|} \right) \right) \right) &= \\ E_0 \left(\int_0^\infty N_1 \tilde{\epsilon} n_{\tilde{\epsilon}} d\tilde{\epsilon} - \left(\frac{|\Delta|}{2k_B T_c} \right)^2 \left(\frac{1}{2} + \ln \left(\frac{\Delta_0}{|\Delta|} \right) \right) \right) \end{aligned} \quad (21)$$

with $\tilde{\epsilon} = \epsilon/k_B T_c$, $\Delta_0 = 1.76k_B T_c$, $E_0 = 4N(0)(k_B T_c)^2$.

In numerical calculations we use parameters typical for NbN: $\hbar\omega_D = 30\text{meV}$ (chosen value of $\hbar\omega_D$ is some kind of compromise between variety values known for different phases of NbN [15]), $k_B T_c = 0.86\text{meV}$ ($T_c = 10K$), $T = T_c/2$, $E_{photon}/E_0 V_{init} = 60$ (with $N(0) = 25.5 \text{ eV}^{-1}\text{nm}^{-3}$ [16], $\xi = 4.8\text{nm}$, $d = 4\text{nm}$ it corresponds to $E_{photon} \simeq 1.3\text{eV}$) and neglect escape of nonequilibrium phonons to substrate because usually $\tau_{esc} \gg \tau_{|\Delta|}$.

At time $t \lesssim \tau_{|\Delta|}$ energy of the absorbed photon $\sim 1.3\text{eV}$ is concentrated in relatively small volume $V_{init} \simeq \pi\xi^2 d \pi \simeq 290\text{nm}^3$ which means high energy concentration. The larger the γ the higher is the temperature of both electrons T_e and phonons $T_{ph} = T_e$, as one can see from Eqs. (19-21) if one inserts there Fermi-Dirac and Bose-Einstein functions for n_ϵ and N_ϵ , respectively (these functions null collision integrals when the downconversion cascade is over and one neglects diffusion of electrons). Because electron-phonon relaxation time $\tau_{e-ph}(\epsilon \ll k_B T_e) \simeq T_e^{-3}$ and $\tau_{e-e}(\epsilon \ll k_B T_e) \simeq \alpha_{e-e}^{-1} T_e^{-1}$ one could expect that for relatively large γ and α_{e-e} the energy of optical or near-infrared photon could be shared between electron and phonon systems and electrons with phonons could be thermalized by time $t \simeq \tau_{|\Delta|}$.

To prove it in Fig. 1 we show the time dependence of the energy of the electronic system calculated at different initial conditions, $\gamma = 1 - 100$ and the same injected energy. One can see that for $\gamma = 100$ already by time $\tau_{sh} \simeq 0.001\tau_0$ the largest part of injected energy is shared between electrons and phonons (even in absence of e-e scattering) and τ_{sh} increases with decrease of γ .

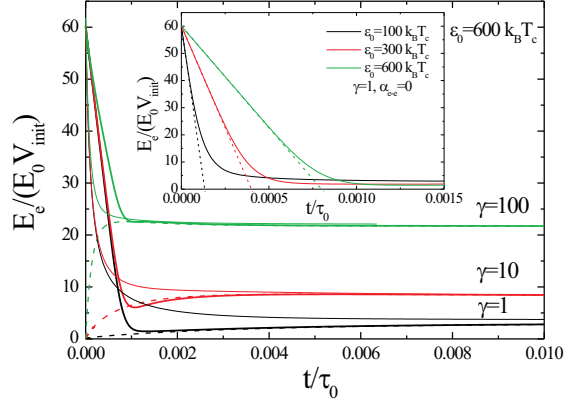


FIG. 1: Dependence of the electronic energy E_e on time found from solution of kinetic equations at different γ and different initial conditions: electron bubble with $\epsilon_0 = 600k_B T_c$, $\alpha_{e-e} = 0$ (solid thick curves), phonon bubble with $\epsilon_0 = 30k_B T_c$, $\alpha_{e-e} = 0$ (dashed curves) and hot electrons with initial $T_e = 8.6T_c$, $\alpha_{e-e} = 1000$ (solid thin curves). In all cases the injected energy to the electrons and phonons is the same and it is equal to $\simeq 1.3\text{eV}$ in the volume $V_{init} = \pi\xi^2 d \simeq 290 \text{ nm}^3$. In the inset we show dynamics of E_e with electron bubble initial condition, $\alpha_{e-e} = 0$ and different ϵ_0 . Dashed lines are linear dependence $E_e = E_{photon}(1 - t/\tau_{leak})$ with τ_{leak} taken from Eq. (22).

Parameter γ controls what part of injected energy goes to electronic system - the larger γ the larger is this part (see Fig. 1).

Sharing time τ_{sh} is actually the thermalization time τ_{th} in electronic and phonon systems. In Fig. 2 we show time evolution of Φ_{neq} (which controls the suppression of $|\Delta|$) at different γ and α_{e-e} . Results are found in case of phonon bubble initial condition. Φ_{neq} practically stops depending on time when electrons are thermalized and n_ϵ is described by Fermi-Dirac function. We fit numerical $\Phi_{neq}(t)$ by the expression $\Phi_{neq}(t \rightarrow \infty)(1 - \exp(-t/\tau_{th}))$ and find τ_{th} (examples of fitting are shown in Fig. 2). One can see that thermalization time decreases with increase of γ (which is consequence of larger energy transfer to electron system) or with increase of α_{e-e} (which is consequence of shorter τ_{e-e}).

In case of electron bubble initial condition and $\epsilon_0 \gg \hbar\omega_D, \delta\epsilon \ll \epsilon_0$ one can find analytical expression for time τ_{leak} during which the energy leaks from electrons to phonons at very beginning of downconversion cascade. Indeed, inserting n_ϵ in form of Eq. (16) in phonon-electron collision integral one finds that $I_{ph-e} \simeq 2\gamma\alpha/(\tau_0 k_B T_c)$ at energies $\epsilon \gg |\Delta|$. Than assuming that α depends on time and the full energy is conserved and is equal to the energy of the photon (we neglect here $E_e^{eq} + E_{ph}^{eq} \ll E_{photon}$) one finds $E_e = E_{photon} \exp(-t/\tau_{leak})$

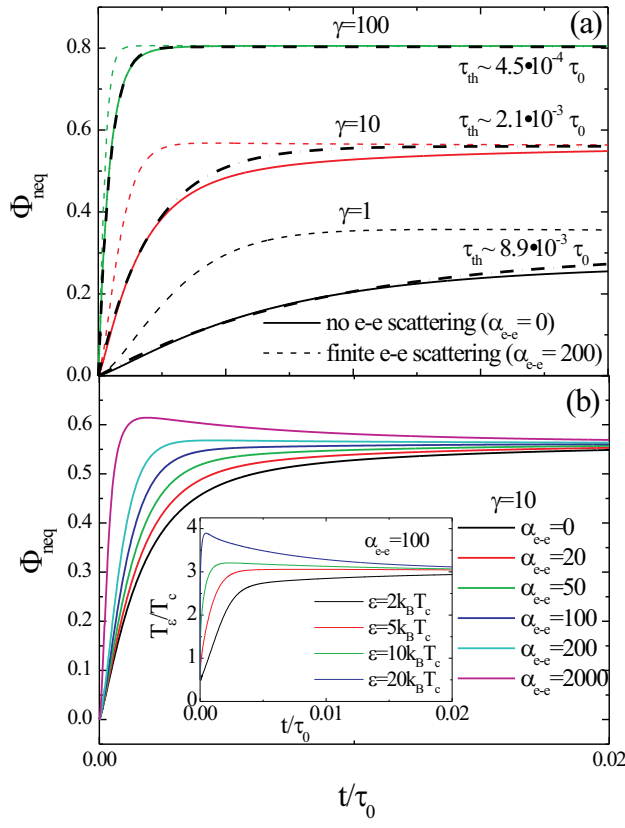


FIG. 2: (a) Time evolution of Φ_{neq} at different γ and two values of α_{e-e} . Fitting $\Phi_{neq}(t)$ (when $\alpha_{e-e} = 0$) by expression $\Phi_{neq}(t \rightarrow \infty)(1 - \exp(-t/\tau_{th}))$ is shown by thick dashed curves with corresponding τ_{th} . (b) Time evolution of Φ_{neq} at $\gamma = 10$ and different α_{e-e} . All results are obtained for phonon bubble initial condition and $T = T_c/2$. In inset of figure (b) we present time evolution of $T_\epsilon = \epsilon/k_B \ln(1/n_\epsilon - 1)$ at different energies and $\gamma = 10$, $\alpha_{e-e} = 100$. At $t=0$, $n_\epsilon = n_\epsilon^{eq}$ and $T_\epsilon = T = T_c/2$ at all energies. After injection of energy to the phonon system n_ϵ deviates from equilibrium which leads to different T_ϵ . $T_\epsilon = T_c \simeq 3T_c$ at all energies at $t \gg \tau_{th} \simeq 1.2 \cdot 10^{-3}\tau_0$.

with

$$\tau_{leak} = \tau_0 \frac{2\epsilon_0(k_B T_c)^3}{(\hbar\omega_D)^4} = \frac{2\epsilon_0\hbar}{g(\hbar\omega_D)^2}. \quad (22)$$

At $t \ll \tau_{leak}$ one has linear decay $E_e = E_{photon}(1 - t/\tau_{leak})$ and it is shown as dashed lines in inset of Fig. 1. For $\gamma = 100$ $\tau_{leak} \simeq \tau_{th}$ and above simple calculations are valid only qualitatively. For $\gamma = 1, 10$ $\tau_{leak} \ll \tau_{th}$ and there is good quantitative agreement between numerical and analytical results at $t \lesssim \tau_{leak}$ (see inset in Fig. 1). When $\tau_{leak} \ll \tau_{th}$ the phonon system absorbs more energy by time $t \simeq \tau_{leak}$ than it should have at $t \gg \tau_{th}$ according to energy conservation law (see Eqs. (19-21)) and it leads to nonmonotonic time dependence of E_e

when $\gamma = 1, 10$ (this effect is absent for $\gamma = 100$ when $\tau_{leak} \simeq \tau_{th}$ - see Fig. 1).

For self-consistency of found τ_{th} the radius of initial hot spot (ξ in our model) should coincide or be smaller than diffusion length of hot electrons $\sim 2\sqrt{D\tau_{th}}$. To make such a comparison one should know τ_0 , γ and α_{e-e} for NbN. Theoretical estimation with help of Eq. (6) and $g = 1$ gives $\tau_0 \simeq 925ps$. τ_0 could be also found if one knows $\tau_{e-ph}(T_c)$ via relation $\tau_0 = 14\zeta(3)\tau_{e-ph}(T_c)$ [9, 21]. In thin NbN film $\tau_{e-ph}(T_c = 10K) \simeq 16ps$ [22] which gives us $\tau_0 \simeq 270ps$. With last value for τ_0 and $R_\square = 500O\text{hm}$ we find $\alpha_{e-e} \simeq 1.8$. Such a small α_{e-e} means (see Fig. 2(b)) that at least at the initial stage of hot spot formation e-e scattering plays small role and downconversion cascade and thermalization occurs mainly via electron-phonon and phonon-electron scattering. Our estimation of $\gamma = 9$ for NbN is based on $N_{ion} = 4.8 \cdot 10^{22}cm^{-3}$ calculated from molar mass $106.9 g/mol$ and density $\rho = 8.47 g/cm^3$ taken from Wikipedia). Therefore for NbN $\tau_{th} \simeq 2.1 \cdot 10^{-3}\tau_0 \simeq 0.57ps > \tau_{|\Delta|} \simeq 0.42ps$ and radius of initial hot spot $2\sqrt{D\tau_{th}} \simeq 11nm$ more than two times larger than $\xi = 4.8nm$. These calculations show that one cannot expect complete thermalization of electrons and phonons in NbN by time when radius of hot spot becomes about ξ and $E_{photon} = 1.3eV$.

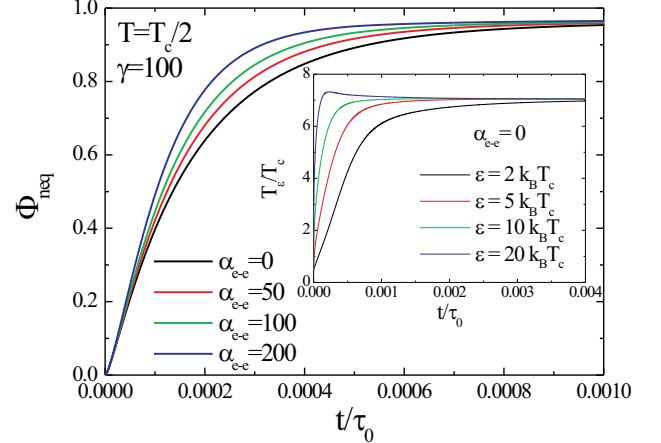


FIG. 3: (a) Time evolution of Φ_{neq} at $\gamma = 100$ and different α_{e-e} . All results are obtained for phonon bubble initial condition, $T = T_c/2$ and parameters of WSi taken from [20]. In inset we present time evolution of $T_\epsilon = \epsilon/k_B \ln(1/n_\epsilon - 1)$ at different energies and $\alpha_{e-e} = 0$. After injection of energy to the phonon system n_ϵ deviates from equilibrium which leads to different T_ϵ . $T_\epsilon = T_c \simeq 7T_c$ at all energies at $t \gg \tau_{th} \simeq 1.9 \cdot 10^{-4}\tau_0$.

We also do calculations for WSi material which demonstrates good ability to detect single photons in optical and near-infrared range [19]. We take parameters of WSi from [20] ($T_c = 3.4K$, $N(0) = 26.5eV/nm^3$,

$\hbar\omega_D = 34\text{meV}$, $D = 0.58\text{cm}^2/\text{s}$, $d = 3.4\text{nm}$). Results are shown in Fig. 3 where we use only phonon bubble initial condition and $\gamma = 100$ which is close to $\gamma = 89$ expected for WSi ($C_e/C_{ph}|_{T_c} = 5.65$ is calculated in Ref. [20] with help of molar mass and density of WSi). In this material $\tau_0 \simeq 10\text{ns}$ if one uses theoretical estimation from [20] or $\tau_0 \simeq 1.9\text{ns}$ as it follows from recent experiment where τ_{e-ph} has been extracted from temperature dependence of magnetoconductivity [23]. We adopt last value and with $R_\square = 595\text{Ohm}$ it gives us $\alpha_{e-e} \simeq 5$. For $E_{photon} = 1.3\text{eV}$ we have $\tau_{th} \simeq 1.9 \cdot 10^{-4}\tau_0 \simeq 0.36\text{ps} \ll \tau_{|\Delta|} \sim 1.3\text{ps}$ for WSi and radius of hot spot $2\sqrt{D\tau_{th}} \simeq 9.1\text{nm}$ is close to coherence length in WSi $\xi \simeq 8.3\text{nm}$ which we use at calculation of V_{init} .

It seems that accounting of diffusion of nonequilibrium electrons at initial stage of hot spot formation (at $t \lesssim \tau_{|\Delta|}$) should only decrease τ_{th} . Indeed, volume of hot spot $V \ll V_{init}$ at times $t \ll \tau_{|\Delta|}$ which leads to higher energy concentration and, hence, faster thermalization.

It is obvious that τ_{th} depends on energy of the photon and V_{init} . This thermalization time could be estimated without solution of kinetic equations with help of energy conservation law (Eq. (19)) and if one associates τ_{th} with $\tau_{e-ph}(T_e)$ for electrons having energy $\epsilon \ll k_B T_e$. Assuming that electron and phonon distribution functions are described by Fermi-Dirac and Bose-Einstein expressions with $T = T_e = T_{ph}$ from Eq. (20,21) one finds Eqs. (24,25) of section IV. For parameters of NbN and WSi materials from Eqs. (19,24,25) it follows that absorption of photon with energy 1.3 eV in chosen volume $V_{init} = \pi\xi^2 d$ heats locally electrons and phonons up to temperature $T_e = T_{ph} \simeq 3T_c$ and $T_e = T_{ph} \simeq 7T_c$, respectively, which is close to results of numerical calculations (see insets in Figs. 2b, 3). $\tau_{e-ph}(T_e)$ could be expressed via τ_0 as $\tau_{e-ph}(T_e) = \tau_0/(14\zeta(3))(T_c/T_e)^3$ [9, 21] which gives $\tau_{th} = \tau_{e-ph}(T_e) \simeq 2.2 \cdot 10^{-3}\tau_0$ and $1.8 \cdot 10^{-4}\tau_0$ for these materials, which is again close to numerical results.

We did the same calculations for normal metal (we put $|\Delta| = 0$, which in the experiment could be done by application of relatively large magnetic field) and found very similar results. This is not surprising, because at times $t \ll \tau_{leak}$ deviation from equilibrium occurs at the energies much larger than $|\Delta|$, while at $t > \tau_{th}$ main contribution to collision integrals comes from energies $\epsilon \simeq k_B T_e \gg |\Delta| \simeq 1.76k_B T_c$ (see insets in Figs. 2, 3) where spectral functions N_1 and R_2 are close to their values in the normal state. We also expect weak dependence on the bath temperature (if it varies in range $0 \lesssim T \lesssim T_c$) because of large injected energy, which provides local heating of electrons and phonons up to $T_e \gg T_c$.

We have to stress that our results are valid only at times $t \lesssim \tau_{|\Delta|}$ when the volume of the hot spot is smaller than $V_{init} = \pi\xi^2 d$. At larger times $t \gtrsim \tau_{|\Delta|}$ shown in Figs. 1-3 results should be considered only as a precursor for consequent dynamics of E_e and Φ_{neq} . To study the evolution of hot spot at time $t \gtrsim \tau_{|\Delta|}$ we consider two limits. In the first limit, limit of long thermalization

time $\tau_{th} \sim \tau_{D,w} \gg \tau_{|\Delta|}$ ($\tau_{D,w} \simeq w^2/16D - w^2/4D \simeq 12.5 - 50\text{ps}$ for strip with $w = 100\text{nm}$ and $D = 0.5\text{cm}^2/\text{s}$, depending where photon is absorbed - in the center or at the edge of the strip), it is assumed that the largest impact on superconducting properties occurs when hot electrons reach both edges of the strip and simultaneously they become thermalized. We expect such a situation in superconductors with small $D \lesssim 1\text{cm}^2/\text{s}$ and $\gamma \leq 1$ or in materials with relatively large $\gamma > 1$ and large diffusion coefficient $D \gg 1\text{cm}^2/\text{s}$. Because usually $\tau_{D,w} \gg \tau_{|\Delta|}$ we expect that $|\Delta|(t)$ changes with $\Phi_{neq}(t)$ instantly and by time $t \simeq \tau_{D,w}$ one has hot belt - region with heated electrons and phonons up to temperature $T_e = T_{ph} > T$ and partially suppressed $|\Delta|(T_e)$ across whole width of the strip (see Fig. 4(a)). To calculate T_e and to find the critical current of the strip with hot belt one can use energy conservation law and this problem is considered in section IV.

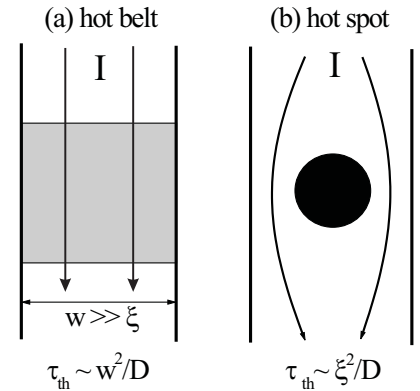


FIG. 4: Sketch of two situations, depending on the value of thermalization time τ_{th}

In the second limit, limit of short thermalization time $\tau_{th} \lesssim \tau_{|\Delta|}$, Φ_{neq} reaches maximal value already in short time interval after energy injection (see Fig. 2) when the radius of hot spot $R_{HS} \sim \xi \ll w$ (we expect that it is realized in superconductors with relatively small $D \lesssim 1\text{cm}^2/\text{s}$ and large $\gamma \gtrsim 100$). Due to diffusion of electrons T_e decreases (and Φ_{neq} decreases too) inside the hot spot but while $T_e > T_c$ and $R_{HS} \gg \xi$ the order parameter in the hot region is strongly suppressed. It provides large current crowding effect around hot spot (superconducting current avoids region with suppressed Δ) and current-carrying state may become unstable before hot electrons reach both edges of the strip (this situation is shown in Fig. 4(b)). We study dynamics of Δ in this limit using modified time-dependent Ginzburg-Landau equation. We also introduce effective temperature of electrons and phonons and solve heat conductance

equations instead of Eqs. (1,2). This limit is studied in section V.

IV. HOT BELT MODEL

In the hot belt model we assume that hot electrons are thermalized among themselves and with phonons by the time when they reach edges of the strip and form a hot belt with size $\sim w \times w$ and with local temperature $T_e = T_{ph} > T$. As a result the critical current of the strip becomes equal to $I_c(T_e)$ because the width and length of the belt $\sim w \gg \xi$ and proximity effect from the regions next to the belt, where $|\Delta|(T) > |\Delta|(T_e)$, could be neglected. We also assume that escape time of nonequilibrium phonons to substrate $\tau_{esc} \gg \tau_{D,w}$. The effective temperature T_e may be determined at given bath temperature T and energy of the photon from the energy conservation law

$$\frac{E_{\text{photon}}}{E_0 w^2 d} = (\mathcal{E}_e(T_e) + \mathcal{E}_{ph}(T_e)) - (\mathcal{E}_e(T) + \mathcal{E}_{ph}(T)) \quad (23)$$

where $\mathcal{E}_{ph}(T)$ is the dimensionless energy of phonon system per unit of volume

$$\mathcal{E}_{ph}(T) = \frac{1}{\gamma} \int_0^{\hbar\omega_D/k_B T_c} \tilde{\epsilon}^3 N_{\tilde{\epsilon}} d\tilde{\epsilon} = \frac{1}{\gamma} \frac{\pi^4}{15} \left(\frac{T}{T_c} \right)^4, \quad (24)$$

(we use that $\hbar\omega_D/k_B T_c \gg 1$ and $N_{\tilde{\epsilon}}$ is described by Bose-Einstein function). In Eq. (23) $\mathcal{E}_e(T)$ is the dimensionless electronic energy per unit of volume

$$\begin{aligned} \mathcal{E}_e(T) &= \int_{|\Delta|/k_B T_c}^{\infty} \tilde{\epsilon} N_1 n_{\tilde{\epsilon}} d\tilde{\epsilon} \\ &- \left(\frac{|\Delta|}{2k_B T_c} \right)^2 \left(\frac{1}{2} + \ln \left(\frac{\Delta_0}{|\Delta|} \right) \right) = \frac{\pi^2}{12} \left(\frac{T}{T_c} \right)^2 - \mathcal{E}_s(T) \end{aligned} \quad (25)$$

where $n_{\tilde{\epsilon}}$ is described by Fermi-Dirac function, for N_1 we use Eq. (13) and

$$\begin{aligned} \mathcal{E}_s(T) &= \int_0^{|\Delta|/k_B T_c} \tilde{\epsilon} n_{\tilde{\epsilon}} d\tilde{\epsilon} - \int_{|\Delta|/k_B T_c}^{\infty} \tilde{\epsilon} (N_1 - 1) n_{\tilde{\epsilon}} d\tilde{\epsilon} \\ &+ \left(\frac{|\Delta|}{2k_B T_c} \right)^2 \left(\frac{1}{2} + \ln \left(\frac{\Delta_0}{|\Delta|} \right) \right), \end{aligned} \quad (26)$$

is the gain in the energy of electrons due to their transition to the superconducting state at $T < T_c$ ($\mathcal{E}_s(T) = 0$ at $T > T_c$).

For practical purposes one may use following interpolation expressions for $\mathcal{E}_s(T)$ and $|\Delta|(T)$

$$\begin{aligned} \mathcal{E}_s(T) &= \left(\frac{|\Delta|(T)}{2k_B T_c} \right)^2 \left(1 - 0.053 \left(\frac{|\Delta|(T)}{k_B T_c} \right)^2 \right. \\ &\left. - 0.1 \left(\frac{|\Delta|(T)}{\Delta_0} \right)^4 - 0.236 e^{-12(1-|\Delta|(T)/\Delta_0)^{0.7}} \right), \end{aligned} \quad (27)$$

$$|\Delta|(T) = 1.76 k_B T_c \tanh(1.74 \sqrt{T_c/T - 1}), \quad (28)$$

which satisfy Eqs. (9, 10, 26) with accuracy better than 2%. Note, that maximal value of \mathcal{E}_s is reached at about $T = T_c/2$, where $\mathcal{E}_s^{\max} \simeq 1/2$.

In presence of the superconducting current \mathcal{E}_s decreases with maximal change at $I = I_{\text{dep}}(T)$. This effect could be taken into account only numerically and it leads to small quantitative difference to the results present in Figs. 5, 6. Here we neglect it.

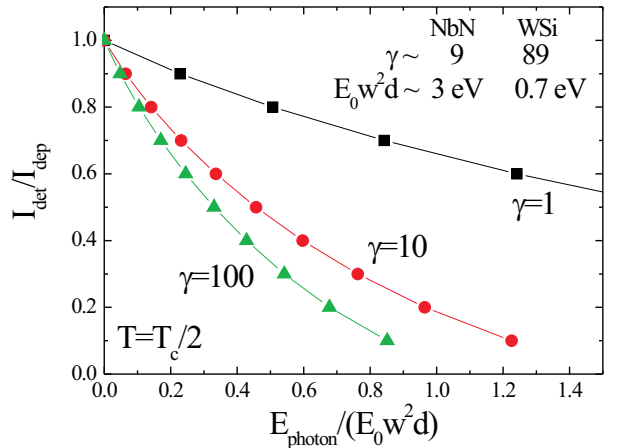


FIG. 5: Dependence of the detection current on the photon's energy at different γ and bath temperature $T = T_c/2$ calculated in hot belt model with help of Eqs. (23-29). In the inset we present expected γ and $E_0 w^2 d$ for NbN and WSi based detectors (with $d = 4\text{nm}$, $w = 100\text{nm}$ and $d = 3.4\text{nm}$, $w = 150\text{nm}$, respectively).

To calculate at which threshold (we call it detection I_{det}) current the photon drives the superconducting strip to the resistive state one needs to know the temperature dependent critical current, which is equal to $I_{\text{dep}}(T_e)$ in our model and for simplicity we adopt Bardeen expression

$$I_{\text{det}} = I_{\text{dep}}(T_e) = I_{\text{dep}}(0) \left(1 - \left(\frac{T_e}{T_c} \right)^2 \right)^{3/2}. \quad (29)$$

With Eqs. (23-29) it is easy to find how detection current changes with photon's energy at given T and γ . Examples of these dependencies are shown in Fig. 5. With increasing γ detection current drastically decreases and at large γ practically does not depend on it, because almost all energy of the photon goes to electronic system when $\gamma \gg 1$. At $\gamma \lesssim 1$ only small fraction of photon's energy goes to the electronic system and detection current is about I_{dep} for considered photon's energies.

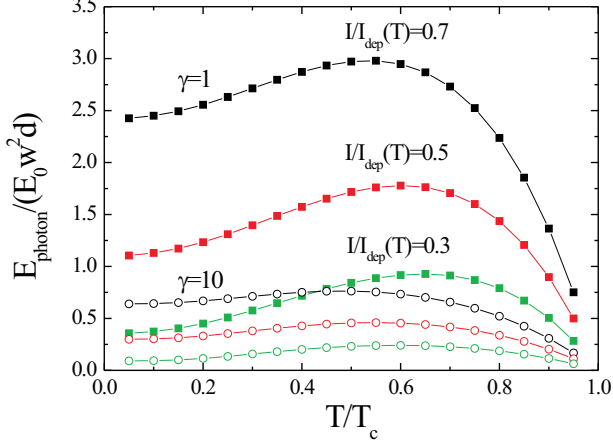


FIG. 6: Dependence of energy of the photon E_{photon} , whose absorption drives the superconducting strip to resistive state, on temperature for $I/I_{\text{dep}}(T) = 0.3, 0.5, 0.7$ and $\gamma = 1, 10$. Calculations are made in framework of hot belt model.

If we fix the ratio $I/I_{\text{dep}}(T)$ the energy of the photon E_{photon} , whose absorption drives the superconducting strip to the resistive state, changes nonmonotonically with temperature (see Fig. 6). The nature of the effect could be easily understood with help of Fig. 7. In this figure we present $I_{\text{dep}}(T)$ (solid curve) and show how much one should increase the temperature (by δT) in the hot belt to transfer the strip to the resistive state at three different temperatures and $I/I_{\text{dep}}(T) = 0.5$. δT decreases with increase of T but due to nonlinear temperature dependence $\mathcal{E}_e(T)$ and $\mathcal{E}_{ph}(T)$ to heat the strip from $T = 0.5T_c$ up to $0.74 T_c$ takes more energy than from $T = 0$ up to $T = 0.61T_c$. Because $\delta T \rightarrow 0$ as $T \rightarrow T_c$ there is a local maxima in dependence $E_{\text{photon}}(T)$ (position of maxima depends on γ and I/I_{dep} - see Fig. 6).

In above consideration we assume that at $I > I_{\text{det}}$ expanding normal domain appears in the superconducting strip, which leads to relatively large voltage signal in contemporary SNSPD. It is well known that below some retrapping current $I_r(T)$ the normal domain cannot expand and shrinks in the current carrying strip [24, 25]. Therefore, to see the voltage signal in existed SNSPD the current in the strip should, at least, exceed I_r . It means that for relatively large photon's energies, when formal I_{det} , calculated from above equations, becomes smaller than $I_r(T)$ real $I_{\text{det}} \gtrsim I_r$ and it should not depend on E_{photon} . Support of this idea could be found in Ref. [26] were WSi-based SNSPD was studied. In Fig. 3(a) of that work dependence of photon detection efficiency (DE) on current is present at different temperatures. One can see that in wide temperature interval DE starts to increase at the current which weakly depends on the tempera-

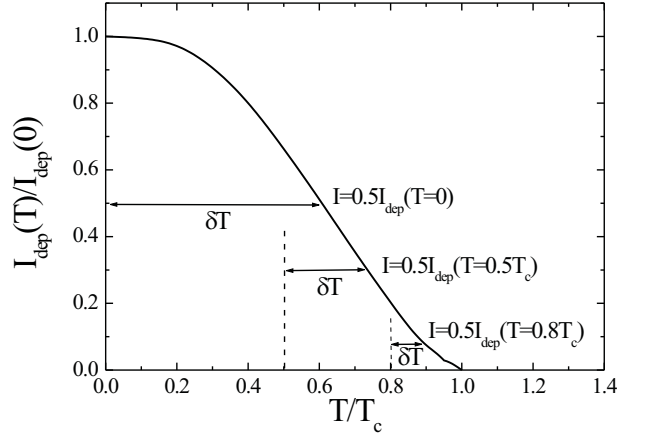


FIG. 7: Figure illustrates how much one should increase the temperature in the hot belt region (at three different bath temperatures $T = 0, 0.5T_c, 0.8T_c$ and three currents $I = I_{\text{dep}}(T)/2$) to drive the superconducting strip to the resistive state.

ture. This resembles weak temperature dependence of I_r at relatively low temperatures (see for example Fig. 7(b) in [25]) in contrast with noticeable temperature dependence of the critical (switching) current in the same temperature interval (compare Fig. 3(a) of Ref. [26] with Fig. 7(b) of Ref. [25]).

Due to the same reason one should treat results shown in Fig. 6 carefully at temperatures close to T_c . As $T \rightarrow T_c$ retrapping current approaches depairing (critical) current and at some temperature $I_r = I_{\text{dep}}$ (in Ref. [25] it occurs at $T \simeq 0.82T_c$). Therefore, results present in Fig. 6 are valid while current is larger than $I_r(T)$.

Let's make estimations for NbN and WSi. Product $E_0 w^2 d \simeq 3\text{ eV}$ and $\gamma \sim 9$ in case of NbN strip with $w = 100$ nm and $d = 4$ nm. For WSi strip $E_0 w^2 d \simeq 0.7\text{ eV}$ and $\gamma \sim 89$ ($w = 150$ nm, $d = 3.4$ nm). According to Fig. 5 at current $I = I_{\text{dep}}/2$ and temperature $T = T_c/2$ NbN strip would be able to detect single photons with energy 1.35 eV, while WSi strip can detect photons with much smaller energy 0.23 eV, if one believes that hot belt model is valid for these materials and $\tau_{\text{esc}} \gg \tau_{D,w}$.

V. HOT SPOT TWO-TEMPERATURE MODEL

In this section we study limiting case of short thermalization time $\tau_{\text{th}} \simeq \tau_{|\Delta|}$ at the initial stage of hot spot formation. Due to diffusion of hot electrons (one may neglect diffusion of hot phonons due to their much lower group velocity in comparison with one for electrons) concentration of absorbed photon's energy in the hot spot with radius $R_{HS} > d$ decreases as $1/R_{HS}^2$. But because

$\mathcal{E}_e \sim T_e^2$ (see Eq. (25)) and $\mathcal{E}_{ph} \sim T_{ph}^4$ (see Eq. (24)) the temperature of electrons drops weaker than $\sim 1/R_{HS}$. One also should have in mind that with decreasing of T_e and T_{ph} the major part of photon's energy goes to the electronic system - due to faster decrease of \mathcal{E}_{ph} in comparison with \mathcal{E}_e .

From another side diffusion time $\tau_D \sim R_{HS}^2/4D$ increases and one can expect that during diffusion the nonequilibrium electrons have time for their thermalization and electron distribution function could be described by the Fermi-Dirac function with effective temperature $T_e \neq T$. Indeed, when $T_e \simeq T_c$ diffusion of hot electrons is impeded due to large $|\Delta| \simeq \Delta_0 \simeq 1.76k_B T_c$ outside the hot spot which should favor thermalization of electrons.

In NbN electrons and phonons are not thermalized on time scale $\lesssim \xi^2/4D$ (see section 3). However difference between diffusion time and thermalization time is not huge and one can expect that despite absence of full thermalization Φ_{neq} is relatively strong inside the growing hot spot to suppress $|\Delta|$ substantially. Indirect prove of this idea comes from the experiment with a magnetic field [34] which validates hot spot model with strongly suppressed $|\Delta|$ in this material. From quantitative point of view usage of 2T model for NbN leads to smaller value of detection current (at fixed energy of the photon) due to stronger suppression of $|\Delta|$ inside the hot spot in comparison with the situation when electrons are not fully thermalized.

In absence of phonon-phonon interaction thermalization of phonons occurs only via electron-phonon and phonon-electron scattering. Our study of initial stage of hot spot formation demonstrate dependence of dynamics of Φ_{neq} only on the value of injected energy to the phonon system but not on the way how it is injected (via phonon bubble or phonon plateau initial conditions). To account the energy adopted by the phonon system during diffusion of electrons we assume that phonon distribution function is described by the Bose-Einstein expression with phonon temperature T_{ph} which, in general, could be different from T_e .

With above assumptions from Eqs. (1-4) one can derive (in a way how it was done in Ref. [27] for normal metal) equations for dynamics of electron and phonon temperatures

$$\begin{aligned} \frac{\partial}{\partial t} \left(\frac{\pi^2 k_B^2 N(0) T_e^2}{3} - E_0 \mathcal{E}_s(T_e, |\Delta|) \right) = \\ = \nabla k_s \nabla T_e - \frac{96\zeta(5)N(0)k_B^2}{\tau_0} \frac{T_e^5 - T_{ph}^5}{T_c^3} + \vec{j} \vec{E}, \quad (30) \end{aligned}$$

$$\frac{\partial T_{ph}^4}{\partial t} = -\frac{T_{ph}^4 - T^4}{\tau_{esc}} + \gamma \frac{24\zeta(5)}{\tau_0} \frac{15}{\pi^4} \frac{T_e^5 - T_{ph}^5}{T_c}, \quad (31)$$

where k_s is a heat conductivity in the superconducting state

$$k_s = k_n \left(1 - \frac{6}{\pi^2 (k_B T_e)^3} \int_0^{|\Delta|} \frac{e^2 e^{\epsilon/k_B T_e} d\epsilon}{(e^{\epsilon/k_B T_e} + 1)^2} \right), \quad (32)$$

$k_n = 2D\pi^2 k_B^2 N(0) T_e / 3$ is a heat conductivity in the normal state and last term in Eq. (30) describes Joule

dissipation (\vec{j} is a current density and \vec{E} is an electric field). In superconducting state in Eq. (30) there are also additional terms, proportional to the charge imbalance $Q \sim \phi + 2e\varphi/\hbar$ and superconducting current density \vec{j}_s , but their effect is small in comparison with Joule dissipation and we skip them.

Note, that when both $|\Delta|$ and T_e vary on time scale comparable with $\tau_{|\Delta|}$, $|\Delta|$ is not determined by T_e via Eq. (10) or Eq. (27) and for \mathcal{E}_s in Eq. (30) one has to use Eq. (26) with independent time-dependent variables $T_e(t)$ and $|\Delta|(t)$. As a physical consequence, variation of $|\Delta|$ leads to heating or cooling of electrons [28] depending on sign of $\partial|\Delta|/\partial t$.

At derivation of Eqs. (30-32) we use Eqs. (13,14) for N_1 and R_2 and we put $M = 1$ in I_{e-ph} and I_{ph-e} which is strictly valid when $|\Delta| = 0$. In the superconducting state $M \neq 1$ and it leads to increase of τ_{e-ph} and, hence, process of cooling of electrons via their coupling with phonons becomes longer. But because cooling of electrons is faster due to diffusion (usually $\tau_{e-ph}(T_c) > \tau_{D,w}$) we do not expect large influence of this effect, at least on time scale $t < \tau_{D,w}$.

For normal metal with $T_{ph} = T$ Eq. (30) was obtained in Refs. [27, 29] and in limit $|T_{e,ph} - T| \ll T$ above equations with zero gradient terms coincide with Eqs. (13, 14) present in Ref. [30].

Appearance of the hot spot (region with suppressed $|\Delta|$) in the strip leads to current redistribution. To find out current distribution in each moment in time one has to solve equation $\text{div} \vec{j} = 0$, where current density $\vec{j} = \vec{j}_s + \vec{j}_n$ consists, in general, of superconducting \vec{j}_s and normal \vec{j}_n parts. Superconducting current in the dirty (Usadel) limit is described by following expression

$$\begin{aligned} \vec{j}_s^{Us} = \frac{\sigma_n}{e\hbar} \vec{q}_s \int_0^\infty 2N_2 R_2 (1 - 2n_\epsilon) d\epsilon \simeq \\ \simeq \frac{\pi\sigma_n}{2e\hbar} |\Delta| \tanh \left(\frac{|\Delta|}{2k_B T_e} \right) \vec{q}_s, \quad (33) \end{aligned}$$

where $\sigma_n = 2e^2 D N(0)$ is the normal state conductivity.

The last expression in Eq. (33) is obtained in the limit of small $|q_s| \ll q_s^{dep}$, omitting spatial derivative in Eq. (9) (in this case $2N_2 R_2 = \pi\delta(\epsilon - |\Delta|)/2$, where $\delta(x)$ is Dirac function) and when for n_ϵ one uses Fermi-Dirac function. It turns out that this expression gives good approximation for \vec{j}_s^{Us} at all $|q_s|$ and we use it in our calculations. When $k_B T_e \gg |\Delta|$ from Eq. (33) one can derive well-known expression for j_s in Ginzburg-Landau model

$$\vec{j}_s^{GL} = \frac{\pi\sigma_n |\Delta|^2}{4ek_B T_c \hbar} \vec{q}_s. \quad (34)$$

For normal component of the current density we adopt simplified expression

$$\vec{j}_n = -\sigma_n \nabla \varphi, \quad (35)$$

(φ is the electrostatic potential) which follows from more general expression (see for example Refs. [31, 32]) in the

limit $k_B T_e \gg |\Delta|$. Note, that the normal current density has large value (comparable or larger than j_s) only in the region with suppressed $|\Delta|$, which approves our choice.

To calculate effect of $n_e \neq n_e^{eq}$ or $T_e \neq T$ on $|\Delta|$ we use modified time-dependent Ginzburg-Landau equation which describes dynamics of complex order parameter $\Delta = |\Delta|e^{i\phi}$. Eq. (10) is not convenient for studying the situation when vortex (or vortices) appears in the superconducting system, because strictly in the center of the vortex $|\Delta| = 0$, $|\vec{q}_s| = \infty$ and there is non zero vorticity $\oint \nabla \phi dl = \pm 2\pi$ (+ for vortex and - for antivortex). It is more convenient to deal with an equation which operates with complex order parameter where vortices appear naturally. Unfortunately, usual Ginzburg-Landau (GL) equation is quantitatively valid only near T_c . Therefore we modify coefficients at spatial derivative and at nonlinear term ($|\Delta|^2$) in GL equation to have temperature dependence $|\Delta|(T)$ and $\xi(T)$ close to correct one at all temperatures

$$\frac{\pi \hbar}{8k_B T_c} \left(\frac{\partial}{\partial t} + \frac{2ie\varphi}{\hbar} \right) \Delta = \xi_{mod}^2 \left(\nabla - i \frac{2e}{\hbar c} A \right)^2 \Delta + \left(1 - \frac{T_e}{T_c} - \frac{|\Delta|^2}{\Delta_{mod}^2} \right) \Delta + i \frac{(div \vec{j}_s^{Us} - div \vec{j}_s^{GL})}{|\Delta|} \frac{\hbar D}{\sigma_n \sqrt{2} \sqrt{1 + T_e/T_c}}, \quad (36)$$

where $\xi_{mod}^2 = \pi \sqrt{2} \hbar D / (8k_B T_c \sqrt{1 + T_e/T_c})$, $\Delta_{mod}^2 = (\Delta_0 \tanh(1.74 \sqrt{T_c/T_e - 1}))^2 / (1 - T_e/T_c)$, A is the vector potential. When $T_e \rightarrow T_c$ coefficients ξ_{mod}^2 and Δ_{mod}^2 go to familiar GL coefficients in the dirty limit. We check that Eq. (36) together with Eq. (33) give the depairing current close to one which follows from the dirty limit at all temperatures (the largest deviation < 5% occurs at $T = 0$) in contrast with Ginzburg-Landau depairing current. Last term in right hand side of Eq. (36) provides conservation of the superconducting current in the stationary state with $\dot{\phi} + 2e\varphi/\hbar = 0$: $div \vec{j}_s^{Us} = 0$. If we do not include this term the stationary solution of Eq. (36) leads to $div \vec{j}_s^{GL} = 0$. Presence of hot electrons is reflected in Eq. (36) via $T_e \neq T$ whose effect on $|\Delta|$ is analogical to effect of $\Phi_{neg} \neq 0$ in Eq. (10).

In the framework of the considered model the electrostatic potential should be found from the current conservation law

$$div \vec{j}_n = -\sigma_n \nabla^2 \varphi = -div \vec{j}_s^{Us}, \quad (37)$$

Eqs. (30, 31, 36, 37) are solved numerically for 2D superconducting strip of finite width $w = 20\xi_c$ and length $L = 4w = 80\xi_c$. $\xi_c^2 = \hbar D / k_B T_c \simeq 1.8 \xi_{mod}^2 (T_e = 0)$ is a natural length scale in Usadel equation when the energy is scaled in units of $k_B T_c$ and we keep it for modified GL equation too. At the transverse edges we use boundary conditions $\vec{j}_n|_n = \vec{j}_s|_n = 0$ and $\partial T_e / \partial n = 0$, $\partial |\Delta| / \partial n = 0$ while at the longitudinal edges: $T_e = T$, $|\Delta| = 0$, $\vec{j}_s|_n = 0$, $\vec{j}_n|_n = I/wd$. The latter boundary

conditions model contact of the superconducting strip with a normal reservoir being in equilibrium. This choice is not explained by any physical reason but it is connected with the simplest way 'to inject' the current to the superconducting strip in numerical modelling.

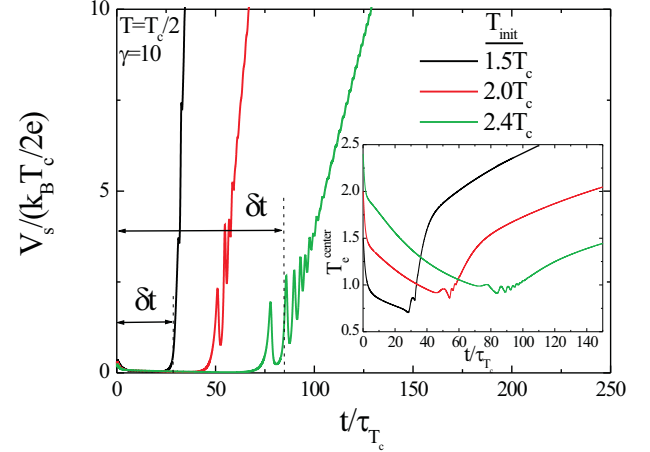


FIG. 8: Time dependence of voltage along superconducting strip V_s and electron temperature in the center of hot spot T_e^{center} (see the inset) calculated for different T_{init} . At $t = 0$ the initial hot spot appears in the center of the strip and I is slightly larger than I_{det} for corresponding T_{init} (see Fig. 9). At $t \gtrsim \delta t$ there is rapid growth of the voltage because of expansion of normal domain. Oscillations in V_s and T_e^{center} are connected with nucleation and passage of vortices and antivortices across the strip.

In numerical calculations we scale time in units $\tau_{T_c} = \hbar/k_B T_c$ which is proportional to $\tau_{|\Delta|}$ at low temperatures. We choose $\tau_0 = 900ps \simeq 1184\tau_{T_c}$ which corresponds to our theoretical estimation for NbN with $T_c = 10K$ (see discussion in section III). We check that results change slightly with increase or decreases of τ_0 because main cooling of hot electrons is due to their diffusion and not their coupling to phonons (which is controlled by τ_0), at least at times $t \lesssim w^2/4D$.

Based on results of section III we assume that after absorption of the photon by the strip the hot spot with size $2\xi_c \times 2\xi_c$ appears with $T_{e,ph} = T_{init} > T$ inside the hot spot and $T_{e,ph} = T$ outside it, while $|\Delta| = |\Delta|(T)$ everywhere. With this initial condition at $t = 0$ we study the dynamics of Δ and $T_{e,ph}$ in the strip. In our calculations we put $\tau_{esc} = \infty$ (effect of finite τ_{esc} is discussed in Sec. VI).

We found that for any $T_{init} > T$ there is a threshold current (we call it as a detection current I_{det}) above which the normal domain nucleates and expands in the strip after appearance of the initial hot spot. Mechanism of destruction of superconductivity depends on the position of the initial hot spot in the strip. When it is

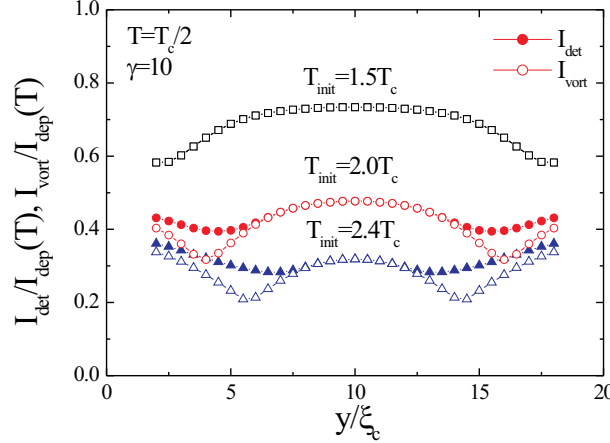


FIG. 9: Dependence of I_{det} (at $I > I_{det}$ normal domain expands in the superconducting strip) and I_{vort} (at $I_{vort} < I < I_{det}$ nucleation and motion of vortices does not lead to appearance of growing normal domain) on coordinate of initial hot spot having size $2\xi_c \times 2\xi_c$ and different T_{init} . $T_{init} = 1.5T_c$ corresponds to absorption of the photon with energy $E_{photon} \simeq 30.5E_0\xi_c^2d \simeq 0.38eV$, ($T_{init} = 2.0T_c \rightarrow E_{photon} \simeq 83.8E_0\xi_c^2d \simeq 1.04eV$, $T_{init} = 2.4T_c \rightarrow E_{photon} \simeq 162E_0\xi_c^2d \simeq 2.0eV$) by NbN strip with parameters from section III.

located near the edge, at some stage of the hot spot evolution(expansion) the vortex enters the region with suppressed $|\Delta|$ from the nearest edge of the strip and passes through the superconductor. After that the second, third and so on vortices pass through the strip, the electrons are heated because of presence of electric field \vec{E} and diffuse along the strip that leads to expansion of the resistive/normal domain in the superconductor. When initial hot spot is located near the center of the strip the vortex and antivortex nucleate *inside* expanding hot spot, move to opposite edges of the strip and at $I > I_{det}$ the normal domain again spreads in the strip. Time evolution of the voltage drop along the strip and electronic temperature in the center of hot spot located in the center of the strip are shown in Fig. 8 for photons with different energies (different T_{init}) and at current slightly above $I_{det}(T_{init})$.

Note, that moving vortices could be nucleated in the strip with hot spot at smaller current $I = I_{vort} < I_{det}$ but their motion does not lead to appearance of the growing normal domain when $I_{det} \ll I_{dep}$. Instead, after passage of one or several vortices (number of vortices depends on the current) the superconductivity recovers in the strip. It occurs because in the range of the currents $I_{vort} < I < I_{det}$ cooling of hot electrons due to their diffusion outside the moving vortex core (where $|\vec{E}|$ is maximal) is not compensated by their heating due to Joule dissipation $\vec{j}\vec{E} \sim I^2$.

Dependence of both I_{vort} and I_{det} on the coordinate of

initial hot spot and different T_{init} are present in Fig. 9 (for material with $\gamma = 10$). This result qualitatively coincides with one found in quasi-stationary hot spot model (where the present I_{vort} was defined as I_{det}) [5, 34] and resembles experimental result from Ref. [35] (in Ref. [6] nonmonotonous dependence $I_{det}(y)$ was predicted but without two local minima near the edges and in that model vortices enter the strip only via edges). Neither in Refs. [5, 34] or in Ref. [6] heating of the superconductor due to vortex motion and condition for appearance of normal domain has been studied.

As it is discussed in Ref. [5] dependence $I_{det}(y)$ explains monotonic dependence of the detection efficiency of SNSPD on current (when it changes from minimal I_{det} (I_{det}^{min}) up to its maximal value I_{det}^{max}). It is interesting to note that difference $I_{det}^{max} - I_{det}^{min}$ decreases with increase of T_{init} (energy of the photon) which resemble experimental results found for detectors based on WSi (see Fig. 2 in [19]), NbN (see Fig. 1 in [34]) and MoSi (see Figs. 2,4 in [33]). If one does not take into account heating effects and associate I_{det} with I_{vort} then $I_{det}^{max} - I_{det}^{min} = I_{vort}^{max} - I_{vort}^{min}$ increases with increase of the energy of the photon (see Fig. 9 here or Fig. 5 in Ref. [5]).

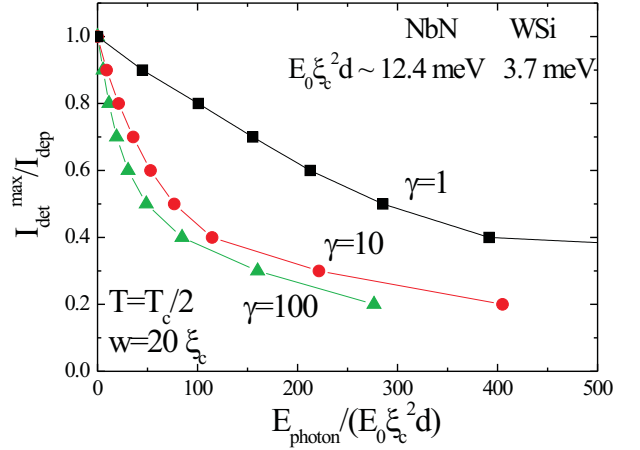


FIG. 10: Dependence of the maximal detection current on the photon's energy at different γ and bath temperature $T = T_c/2$ calculated in 2T hot spot model. Width of the strip $w = 20\xi_c$ ($\xi_c \simeq 6.4nm$ for NbN with $T_c = 10K$ and $\xi_c \simeq 11nm$ for WSi with $T_c = 3.4K$). In the figure we also present value of the product $E_0\xi_c^2d$ for NbN and WSi based detectors with parameters from Sec. III.

When $I > I_{det}^{max}$ detection efficiency reaches maximal value [5]. I_{det}^{max} is located either in the center of the strip or at its edge, depending on T_{init} (see Fig. 9 and compare it with Fig. 5 from [34] and Fig. 4 from [5]). In Fig. 10 we show dependence of I_{det}^{max} on the energy of the photon. Qualitatively Fig. 10 resembles results present

in Fig. 5 for hot belt model but with one important quantitative difference. In case of superconductor with short thermalization time (Fig. 10) one needs smaller current, to detect the single photon or, at fixed current, the photon with smaller energy could be detected than by the strip with large thermalization time (Fig. 5).

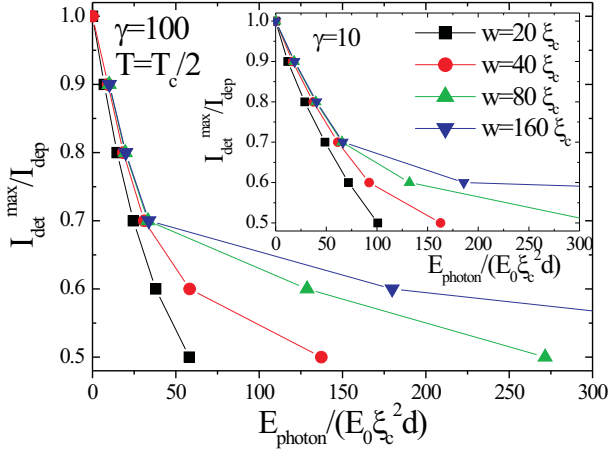


FIG. 11: Dependence of the maximal detection current on photon's energy at $\gamma = 100$ and $\gamma = 10$ (in the inset) calculated in 2T hot spot model for strips with different widths. $I_{\text{det}}^{\text{max}}$ weakly depends on width of the strip when $I_{\text{det}}^{\text{max}}/I_{\text{dep}} \gtrsim 0.7$.

In Fig. 11 we present dependence $I_{\text{det}}^{\text{max}}(E_{\text{photon}})$ for strips with different widths. The most interesting result is that the detection ability of the strip does not depend on its width when $I_{\text{det}}^{\text{max}}/I_{\text{dep}} \gtrsim 0.7$. The effect originates from current crowding around finite size spot with suppressed $|\Delta|$ which leads to instability of superconducting state at $I \lesssim I_{\text{dep}}$ even in the infinitely wide film [2]. Due to magnetic field screening by superconductors (in our calculations we neglect it) this effect exists only in finite width strips with $w \lesssim \Lambda = 2\lambda_L^2/d$ where λ_L is the London penetration depth and screening could be neglected (for NbN film with thickness $d = 4$ nm and $\lambda_L \simeq 450$ nm, $\Lambda \simeq 100\mu\text{m} \simeq 15800\xi_c$). Analytical calculations in London model predict that static normal spot with radius $R \gg \xi$ destroys superconducting state in the infinite film at current $I > 0.5I_{\text{dep}}$ (see Eq. (12) in [2]) while calculations using stationary Ginzburg-Landau equation gives $I \gtrsim 0.7I_{\text{dep}}$ (see inset in Fig. 4 in Ref. [36]). The last result is very close to our finding where in addition we take into account expansion of the hot spot and Joule heating.

As in case of the hot belt model we calculate how depends the energy of the photon, whose absorption drives the strip to the resistive state, on temperature at fixed ratio $I/I_{\text{dep}}(T)$. From Fig. 12 one can see that this dependence is nonmonotonic one as for the hot belt model

(compare Fig. 12 with Fig. 6).

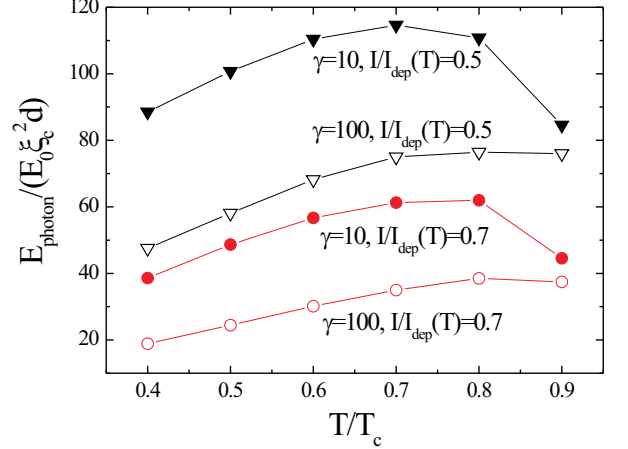


FIG. 12: Dependence of energy of the photon, whose absorption drives the superconducting strip to resistive state, on temperature at $I/I_{\text{dep}}(T) = 0.5, 0.7$ and $\gamma = 10, 100$. Calculations are made in framework of 2T hot spot model.

And, finally, we study effect of the perpendicular magnetic field on I_{det} . Qualitatively results (see Fig. 13) are similar to theoretical findings of Ref. [34], where I_{det} is associated with I_{vort} (compare Fig. 13 with Fig. 6(a) from [34]). The only difference is that in the present model we did not find pinning of the vortices in the strip with $w = 20\xi_c$ at any considered T_{init} (we find that in wider strip expanding hot spot can pin vortices when T_{init} is relatively large). Small variation of $I_{\text{det}}^{\text{min}}$ in case of large T_{init} we mainly connect with weaker Joule heating as current decreases which worsens condition for appearance of growing normal domain. This result correlates with known effect that retrapping current of superconducting strip has much weaker field dependence than its critical current (see for example current-voltage characteristics of NbN strip from Ref. [36]).

VI. DISCUSSION

A. Electron-phonon downconversion cascade

Initial stage of electron-phonon downconversion cascade on time scale of $t \lesssim \tau_{|\Delta|}$ is studied in our work using kinetic equations for spatially uniform system with volume $V_{\text{init}} = \pi\xi^2d \simeq \pi D\tau_{|\Delta|}d$. In comparison with previous works [37, 38] we take into account e-e inelastic scattering and focus on the question how thermalization time τ_{th} and distribution of photon's energy between electronic and phonon systems depend on parameters of superconductor and on time.

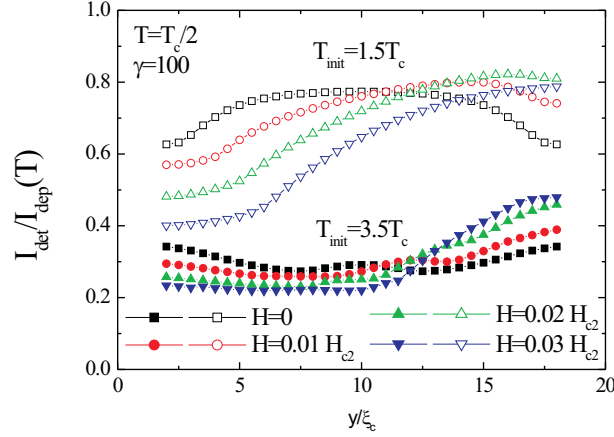


FIG. 13: Dependence of detection current on the position of the initial hot spot across the strip at different magnetic fields and two values of T_{init} corresponding to absorption of photons with different energies ($T_{init} = 1.5T_c \rightarrow E_{photon} \simeq 13.2E_0\xi_c^2d \simeq 0.05\text{eV}$, $T_{init} = 3.5T_c \rightarrow E_{photon} \simeq 124.5E_0\xi_c^2d \simeq 0.46\text{eV}$ for parameters of WSi strip from Sec. III).

By time $t \simeq \tau_{leak}$ (which is about one picosecond for both NbN and WSi materials and $E_{photon} \simeq 1\text{eV}$) part of photon's energy, initially fully absorbed by electrons, leaks to phonons while another fraction stays with electrons. Subsequent dynamics depends on relation between τ_{leak} and τ_{th} . When $\tau_{leak} \ll \tau_{th}$ in time interval $\tau_{leak} < t \lesssim \tau_{th}$ both E_e and E_{ph} nonmonotonically vary in time (with back energy flow from phonons to electrons and vice versa) while at $t \gg \tau_{th}$ they become time-independent. In case of short thermalization time $\tau_{th} \lesssim \tau_{leak}$ such a nonmonotonic dependence is absent and at $t > \tau_{th} \sim \tau_{leak}$ both E_e and E_{ph} practically do not depend on time and electrons are thermalized.

We found both analytically and numerically that τ_{leak} is proportional to the energy of the photon and is inversely proportional to the square of Debye energy. Expression for τ_{leak} (see Eq. (22)) coincides with expression for time τ_1 introduced in Ref. [38] with replacement $3E_1$ by $2\epsilon_0$ ($E_1 \gg \hbar\omega_D$ is determined in [38] as the energy at which $\tau_{e-ph} = \tau_{e-e}$). By time $t \simeq \tau_1$ in model of Ref. [38] practically all energy of the photon is transferred to phonon system. Our calculations show that by time $t \simeq \tau_{leak}$ only part of photon's energy goes to phonons and size of this part depends on parameter γ (see Fig. 1).

Thermalization time depends on γ , strength of e-e scattering and energy of the photon. The larger $\gamma \sim C_e/C_{ph}|T_c$ the larger part of photon's energy finally goes to electrons and shorter τ_{th} . We found that in case of relatively large $\gamma \gtrsim 100$ and $E_{photon} \simeq 1\text{eV}$ thermalization time may be about of leakage time even in absence

of e-e scattering. We also found that for typical low temperature 'dirty' superconducting NbN or WSi films e-e scattering plays no role in electron-phonon energy cascade at $t \lesssim \tau_{|\Delta|}$.

In materials with short $\tau_{th} \simeq \tau_{|\Delta|}$ the electron-phonon downconversion cascade at $t > \tau_{|\Delta|}$ is connected with cooling of electrons and phonons due to diffusion of hot electrons and suppression of $|\Delta|$. We studied this problem assuming complete thermalization of electrons at every step of diffusion process. In this approach suppression of the superconducting order parameter is described solely by $T_e \neq T$ and instability of the superconducting state occurs before the hot electrons reach the both edges of the superconducting strip.

B. Effect of finite escape time and kinetic inductance

In our calculations we neglect energy flow to the substrate, which is controlled by escape time of nonequilibrium phonons τ_{esc} in Eq. (2). One also should keep in mind that in SNSPD current deviates from the superconductor and flow via the shunt when superconducting strip/meander transits to the resistive state. Both effects obviously should increase I_{det} , because decrease of τ_{esc} enhances cooling of electrons while decrease of current weakens Joule heating and it worsens the condition for appearance and expansion of the normal domain. An impression about characteristic time scales could be extracted from Fig. 8. Normal domain expands at $t \gtrsim \delta t$ (at that times voltage grows rapidly) and δt increases with decreasing I_{det} due to decrease of Joule dissipation $\sim I^2$. Therefore, when $\tau_{esc} \lesssim \delta t$ and kinetic inductance of the detector L_k is relatively small, so $L_k/R_s \lesssim \delta t$ (R_s is averaged over time interval $[0, \delta t]$ resistance of the superconductor) these effects must be taken into account. In Fig. 14 we show effect of finite τ_{esc} on the energy-current relation. For large γ escape of nonequilibrium phonons to substrate has less effect on I_{det} because of large ratio $C_e/C_{ph}|T_c$, leading to rise of time of energy transfer from electronic system to phonon one and than to substrate.

C. Current-energy relation

Both hot belt and 2T hot spot model predict nonlinear current-energy relation (see Figs. 5, 10). The nonlinearity at small energies comes from nonlinear temperature dependence of the critical (depairing) current, energy of electron and phonon systems and in case of hot spot model additional nonlinearity comes from current crowding effect around hot spot in the strip with finite width [39]. Nonlinearity at high energies originates from existence of retrapping current, below which normal domain cannot expand in current-carrying superconductors. Therefore at high energies I_{det} should not depend

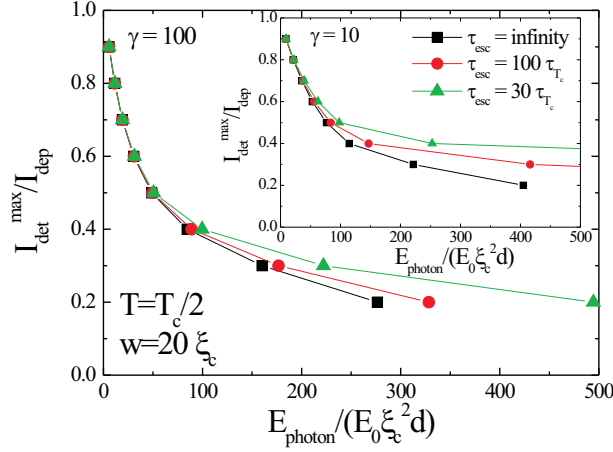


FIG. 14: Dependence of the maximal detection current on the photon's energy at $\gamma = 100$ and different τ_{esc} calculated in 2T hot spot model. In the inset results for $\gamma = 10$ are shown.

on the photon's energy (in modern SNSPD where large voltage signal appears only when large part of superconducting strip converts to the normal state) and it should be about of the retrapping current of the superconducting strip. Retrapping current goes to zero when $\tau_{\text{esc}} \rightarrow \infty$ (when length of the superconductor is much larger than so called healing length [40]) that's why in Figs. 5, 10 there is no saturation of I_{det} at high energies (in that calculations $\tau_{\text{esc}} = \infty$).

In Ref. [41] nonlinear current-energy relation was found (see Fig. 12 there) in the model which resembles our hot belt model. Authors of Ref. [41] assume that electrons are thermalized and become uniformly distributed across the strip soon after photon absorption. The main difference between our hot belt model and approach of [41] is that we explicitly take into account heating of phonons by absorbed photon and for simplicity we neglect effect of the current on the electronic energy in the superconducting state (the last effect should be important for studying multiphoton detection [42] when relaxation of hot spot induced by first photon at large times is determined mainly by electron-phonon inelastic relaxation [41] on the background of large $|\Delta| \gg k_B T_e$). In Ref. [41] the part of the photon's energy which goes to the electronic system is called as energy deposition factor and it is considered as a fitting parameter which does not depend on E_{photon} . From Eqs. (23-25, 29) it follows that part of the photon's energy which goes to the electronic system does depend on E_{photon} due to nonlinear temperature dependencies $\mathcal{E}_e(T)$ and $\mathcal{E}_{\text{ph}}(T)$.

Experimentally nonlinear current-energy relation was observed for NbN, WSi [34] (in inset of Fig. 10 from [34] results for WSi detector are extracted from results of Ref. [19]) and MoSi [33] based detectors. To make

quantitative comparison between theory and experiment one has to know many material parameters, some of them are known ($N(0)$, T_c , R_\square , D) but some of them are not (γ , α_{e-e} , τ_{esc}). The last parameters could be extracted from additional experiments where N_{ion} , ω_D , τ_{e-e} and τ_{esc} could be measured. Calculations of γ for NbN and WSi are based on N_{ion} found from molar mass and density of these materials while Debye frequency is taken either from available experimental data (where it varies for different phases of NbN more than in two times [15]) or it is a result of reasonable estimation [20]. In expression for α_{e-e} we put $a = 1$ (see Eq. (5)) which is not justified by any experiments or rigorous calculations (due to their absence) for NbN and WSi. Taking into account these circumstances and absence of reliable value for τ_{esc} we did not make quantitative comparison with an experiment in our work.

In theoretical paper [6] by A. Engel et. al nearly linear current-energy relation is predicted and in Ref. [43] such a dependence is observed for NbN bridge in large interval of photon's energies (in Ref. [44] current-energy relations for NbN and TaN meanders look as linear ones but they were found in narrow energy interval and could be fitted by nonlinear functions with only one fitting parameter - see Ref. [39]). Experiment shows [45] that for WSi bridge current-energy relation is also nearly linear with small deviation from linear behavior at low energies. The reason for discrepancy between experimental results found in the meander and bridge geometry is not clear at the moment. For example it could be connected with nonuniform current distribution which appears naturally in the bridge those length is comparable with its width. In such a geometry the current density is maximal near edges of the bridge which definitely should affect position dependent detection current and may influence current-energy dependence quantitatively.

D. Temperature-dependent cut-off wavelength

It was found in many experiments, that detection efficiency of SNSPD at fixed current drops very fast at wavelength larger some critical value (it is called as cut-off wavelength λ_c or red boundary wavelength [16, 44]). Systematic measurements of $\lambda_c(T)$ in Ref. [46] reveal that λ_c decreases with increase of the temperature (in considered temperature interval $0.05T_c - 0.6T_c$) when one keeps ratio $I/I_{\text{dep}}(T)$ constant. It is in contrast with naive expectation that as $T \rightarrow T_c$ and $|\Delta|$ decreases one needs lower energy photon (longer wavelength) to destroy superconductivity.

We calculate cut-off photon's energy at different temperatures and fixed ratio $I/I_{\text{dep}}(T)$ in hot belt (see Fig. 6) and 2T hot spot (see Fig. 12) models. Both models predict increase of cut-off energy (decrease of λ_c) with temperature increase when $T \lesssim T_1$ ($T_1 = 0.6T_c - 0.8T_c$ depending on the model, ratio $I/I_{\text{dep}}(T)$ and parameter γ). In both models the effect mainly comes from non-

linear temperature dependence of electronic and phonon energies (see discussion around Fig. 7).

E. Photon detection at temperature near T_c

As $T \rightarrow T_c$ both models predict decrease of cut-off energy (increase of λ_c) in temperature interval $0.6T_c - 0.8T_c \lesssim T < T_c$ when one does not consider expansion of normal domain. When $I < I_r(T)$ the normal domain cannot expand in the superconducting strip and SNSPD should lose ability to detect single photons. Because $I_r(T) = I_c(T)$ ($I_c(T)$ is the critical current of real meander/strip) at some temperature T^* close to T_c the detector cannot detect single photons at $T \gtrsim T^*$. Actually it can stop detecting single photons even at lower temperature. Indeed, retrapping current is determined from the balance between Joule heating and heat removal to the substrate. For relatively short normal domain (with length shorter than thermal healing length η [40]) additional heat removal comes from diffusion of hot electrons from hot spot which increases I_r . From Eqs. (30,31) it follows that the healing length at $T_e \simeq T_c$ and $|T_e - T_c| \ll T_c$ is $\eta = (2\pi^2 D\tau_0 / 1440\zeta(5))^{1/2} / ((1+\alpha)/\alpha)^{1/2}$ where $\alpha = \pi^4 \tau_0 / (450\zeta(5)\gamma\tau_{esc})$. With used parameters of NbN, $\tau_0 = 270\text{ps}$ and $\tau_{esc} \simeq 20\text{ps}$ we find $\alpha \simeq 0.3$ and $\eta \simeq 29\text{nm} \simeq 4.5\xi_c$ which is larger or comparable to the radius of hot spot when it drives the current-carrying superconducting strip to the resistive state (radius of such a hot spot could be extracted for different E_{photon} from Fig. 8 - I_{det} is minimal for hot spot which touches the edge of the strip [5, 34]).

F. Magnetic field as a probe for detection mechanism

Current-energy relation and temperature dependence of cut-off photon's energy following from hot belt and 2T hot spot model are qualitatively the same. To distinguish, which model is related to experiment one needs to make quantitative comparison, but it is difficult to do due to lack of many material parameters. However response of the detector to magnetic field is *qualitatively* different in hot belt and hot spot models. In hot belt model (and any model which assumes uniform, across the strip, distribution of nonequilibrium electrons) applied magnetic field increases detection efficiency at *any* current [34] (or does not change it if DE reaches plateau at high current). In the hot spot model due to position dependent I_{det} weak magnetic field may decrease DE in finite interval of currents [34]. Therefore magnetic field plays the role of qualitative probe for detection mechanism.

G. Single photon detection by micron wide strip

In the hot spot model detection of relatively high energy photon by wide thin strip (with width up to several microns) does not depend on its width if it can carry superconducting current larger than $0.7I_{dep}$ (see Fig. 11 and text around). It brings qualitative difference with hot belt model where detection ability has strong dependence on the width of the strip at any current. Experimental observation of this effect could open the way for new design of SNSPD in form of wide bridge which has much smaller kinetic inductance in comparison with present meander-type detectors and, hence, much shorter voltage pulses. Nowaday detectors based on NbN or TaN have critical current up to $0.6I_{dep}$ [44] which is not high enough (see Fig. 11) for implementation of this idea.

H. Single photon detection by high- T_c superconducting strip

Let us discuss perspectives of high- T_c materials to be used as active element in SNSPD. To simplify situation we use normal spot (NS) model, neglect current crowding effect and position dependence of detection current. In this oversimplified model the radius of normal hot spot could be found from Eq. (23) with replacement $w^2 \rightarrow \pi R^2$, $T_e = T_c$ and assuming that bath temperature $T \ll T_c$ (in this case $\mathcal{E}_s(T) \simeq 0.4$)

$$R_{NS} = \sqrt{\frac{E_{photon}}{4\pi dN(0)(k_B T_c)^2}} \sqrt{\frac{1}{\pi^2/12 + \pi^4/(\gamma 15) + 0.4}} \quad (38)$$

In this model detection current linearly depends on radius of normal spot and does not depend on its position

$$\frac{I_{det}}{I_{dep}} = \left(1 - \frac{2R_{NS}}{w}\right) \quad (39)$$

which is consequence of neglecting current crowding effect and assumption that the photon absorbed near the edge of the strip creates normal spot of the same shape (circle) as the photon absorbed in the center of the strip.

This normal spot model gives order of magnitude correct estimation when current is smaller than $0.5I_{dep}$ (but larger than retrapping current), $R_{NS} \gtrsim w/4$ and effect of current crowding is relatively small (see Fig. 4 in Ref. [36] for comparison of Eq. (39) with numerical result where this effect is taken into account for normal spot located in the center of strip). Indeed, for parameters of NbN based detector from Ref. [34] which demonstrated intrinsic detection efficiency (IDE) about unity at $I/I_{dep} \simeq 0.5$ for photon with wavelength $\lambda = 1000\text{nm}$ (see Fig. 2 in [34]) and $\gamma = 9$ one finds $R_{NS} \simeq 26\text{nm}$ from Eq. (38). With help of Eq. (39) and $w = 100\text{nm}$ it gives us $I_{det}/I_{dep} \simeq 0.5$ which is close to experimental value. But in superconductor with $T_c = 100\text{K}$ and the same other material parameters such a photon will create the

hot spot with radius ten times smaller ($R_{NS} \simeq 2.6\text{nm}$) and one will need strip with width $w \simeq 10\text{nm}$ to detect this photon with IDE $\simeq 1$ at $I = 0.5I_{dep}$. The actual width should be even smaller because parameter $\gamma \sim 1/T_c^2$ (see Eq. (7)) which additionally decreases radius of normal spot.

Situation differs at currents larger than $\sim 0.7I_{dep}$ when energy of the photon weakly depends on width of the strip (see Fig. 11). For example for NbN detector from Ref. [34] and photon with $\lambda = 1000\text{nm}$ ratio $E_{photon}/E_0\xi_c^2 d \simeq 100$ while for superconductor with $T_c = 100\text{K}$ and the same other parameters $E_{photon}/E_0\xi_c^2 d \simeq 10$ which means that one needs current about $0.9 I_{dep}$ to have IDE $\simeq 1$ but with no limit for the width (while it is smaller than Pearl length).

Above arguments show that usage of high- T_c material in SNSPD needs much narrower strip than low- T_c material requires or strip should be of very high quality to have critical current about 90% of depairing current to detect optical or near infrared photon with intrinsic detection efficiency about unity.

VII. CONCLUSION

Our main conclusions are following:

1) After absorption of the near-infrared or optical photon by dirty superconducting strip the thermalization time of both electrons and phonons could be about of time variation of magnitude of superconducting order parameter $\tau_{|\Delta|}$ when the radius of hot spot does not exceed superconducting coherence length. Such a situation could be realized in superconductors with relatively small diffusion coefficient $D \simeq 0.5\text{cm}^2/\text{s}$ and large ratio $C_e/C_{ph}|_{T_c} \gg 1$.

2) At times $t > \tau_{|\Delta|}$ the hot electrons are cooled due to their diffusion, energy exchange with phonons and suppression of $|\Delta|$ inside the expanding hot spot. The larger the energy of the photon the larger is the size of hot spot where local temperature $T_e \gtrsim T_c$ and superconducting state becomes unstable at smaller current.

3) Instability is connected with nucleation and motion of the vortices before the hot spot expands over whole width of the strip. However their motion leads to ap-

pearance of the growing normal domain only at current larger so-called detection current, whose value depends on energy of the photon, place where photon is absorbed, magnetic field and cannot be smaller than retrapping current of the strip.

4) In superconductors with small ratio $C_e/C_{ph}|_{T_c} \ll 1$ detection of near-infrared or optical photon is possible only at current close to depairing current in the strip with width $w \geq 20\xi_c$, because only small fraction of photon's energy goes to electrons. The same we may conclude for superconductors with large diffusion coefficient because in this case the size of hot spot is pretty large by time when electrons are thermalized (hot electrons may form the hot belt across the strip) which leads to locally smaller heating and weaker influence on superconducting properties.

Calculations made for WSi with material parameters available from the literature allows us to conclude that hot belt model should be irrelevant for detectors made from this material and strip with $w = 150\text{nm}$ because $\tau_{D,w} \simeq w^2/16D \simeq 28\text{ps}$ which is much larger than $\tau_{th} \simeq 0.36\text{ps}$ (see Section III). The same conclusion we can make for NbN material despite absence of complete thermalization of electrons at the initial stage of hot spot formation. This conclusion is mainly based on experimental results of Ref. [34] which support the hot spot model with strongly suppressed $|\Delta|$ inside the hot spot. Only for high energy photons, when $I_{det} \ll I_{dep}$ and size of the expanding hot spot, which drives the superconductor to resistive state, is comparable with width of the strip one may expect that hot belt model gives reasonable results. The hot belt model could be also useful for study of two-photon detection [41, 42], when there is time delay between absorption of two photons and hot region can expand over whole width of the superconducting strip.

Acknowledgments

The study is supported by the Russian Foundation for Basic Research (grant No 15-42-02365). D.Yu.V. acknowledges fruitful discussions with Alexander Semenov and Alexander Kozorezov while doing this work.

-
- [1] A. Semenov, A. Engel, H.-W. Hubers, K. Ilin, and M. Siegel, Spectral cut-off in the efficiency of the resistive state formation caused by absorption of a single-photon in current-carrying superconducting nano-strips, *Eur. Phys. J. B* **47**, 495, (2005).
- [2] A. N. Zotova and D. Y. Vodolazov, Photon detection by current-carrying superconducting film: A time-dependent Ginzburg-Landau approach, *Phys. Rev. B* **85**, 024509 (2012).
- [3] L. N. Bulaevskii, M. J. Graf, and V. G. Kogan, Vortex-assisted photon counts and their magnetic field dependence in single-photon superconducting detectors, *Phys. Rev. B* **85**, 014505 (2012).
- [4] A. Eftekharian, H. Atikian, and A. H. Majedi, Plasmonic superconducting nanowire single photon detector, *Opt. Express* **21**, 3043 (2013).
- [5] A. N. Zotova and D. Y. Vodolazov, Intrinsic detection efficiency of superconducting nanowire single photon detector in the modified hot spot model, *Supercond. Sci. Technol.* **27**, 125001 (2014).
- [6] A. Engel, J. Lonsky, X. Zhang, A. Schilling, Detection Mechanism in SNSPD: Numerical Results of a Conceptu-

- ally Simple, Yet Powerful Detection Model, IEEE Trans. Appl. Supercond. **25**, 2200407 (2015).
- [7] A Engel, J J Renema, K Ilin and A Semenov, Detection mechanism of superconducting nanowire single-photon detectors, Supercond. Sci. Technol. **28**, 114003 (2015).
- [8] A. Rothwarf and B. N. Taylor, Measurement of Recombination Lifetimes in Superconductors, Phys. Rev. Lett. **19**, 27 (1967).
- [9] G.M. Eliashberg, Inelastic electron collisions and nonequilibrium stationary states in superconductors, Zh. Eksp. Teor. Fiz. **61**, 1254 (1971).
- [10] A. M. Gulyan and G. F. Zharkov, Electron and phonon kinetics in a nonequilibrium Josephson junction, Sov. Phys. JETP **62**, 89 (1985).
- [11] S.B. Kaplan, C.C. Chi, D.N. Langenberg, J.J. Chang, S. Jafarey and D.J. Scalapino, Quasiparticle and phonon lifetimes in superconductors, Phys. Rev. B **14**, 4854 (1976).
- [12] J.J. Chang and D.J. Scalapino, Kinetic-equation approach to nonequilibrium superconductivity, Phys. Rev. B **15**, 2651 (1977).
- [13] J. Rammer and H. Smith, Field-theoretical methods in transport theory, Rev. Mod. Phys. **58**, 323 (1986).
- [14] B.L. Altshuler, A. G Aronov, Electron-Electron Interaction in Disorder Systems, North-Holland, Amsterdam, Ed. by A. L. Efros and M. Pollock, 1985.
- [15] Y. Zou, X. Wang, T. Chen, X. Li, X. Qi, D. Welch, P. Zhu, B. Liu, T. Cui, and B. Li, Hexagonal-structured ϵ -NbN: ultra-incompressibility, high shear rigidity, and a possible hard superconducting material, Sci. Rep. **5**, 10811 (2015).
- [16] A. Engel, A. Aeschbacher, K. Inderbitzin, A. Schilling, K. Ilin, M. Hofherr, M. Siegel, A. Semenov, and H.-W. Hubers, Tantalum nitride superconducting single-photon detectors with low cut-off energy, Appl. Phys. Lett. **100**, 062601 (2012).
- [17] D. Belitz, Electron-phonon interaction, ultrasonic attenuation, and Eliashberg function $\alpha^2 F(\omega)$ in impure metals, Phys. Rev. B **36**, 2513 (1987).
- [18] V.V. Baranov and V.V. Kabanov, Theory of electronic relaxation in metal excited by an ultrashort optical pump, Phys. Rev. B **89**, 125102 (2014).
- [19] B. Baek, A. E. Lita, V. Verma, and S. W. Nam, Superconducting a-W_xSi_{1-x} nanowire single-photon detector with saturated internal quantum efficiency from visible to 1850 nm, Appl. Phys. Lett. **98**, 251105 (2012).
- [20] M. Sidorova, A. Semenov, A. Korneev, G. Chulkova, Yu. Korneeva, M. Mikhailov, A. Devizenko, A. Kozorezov, G. Goltsman, Electron-phonon relaxation time in ultrathin tungsten silicon film, arXiv:1607.07321.
- [21] A. Schmid and G. Schon, Linearized Kinetic Equations and Relaxation Processes of a Superconductor Near T_c , J. of Low Temp. Phys. **20**, 207 (1975).
- [22] A.D. Semenov, privite communication & A.D. Semenov, R. S. Nebosis, Yu. P. Gousev, M. A. Heusinger, and K. F. Renk, Analysis of the nonequilibrium photoresponse of superconducting films to pulsed radiation by use of a two-temperature model, Phys. Rev. B **52**, 581 (1995).
- [23] X. Zhang, A. Engel, Q. Wang, A. Schilling, A. Semenov, M. Sidorova, H.-W. Hbers, I. Charaev, K. Ilin, and M. Siegel, Characteristics of superconducting tungsten silicide W_xSi_{1-x} for single photon detection, Phys. Rev. B **94**, 174509 (2016).
- [24] M. Tinkham, J. U. Free, C. N. Lau, and N. Markovic, Hysteretic I-V curves of superconducting nanowires, Phys. Rev. B **68**, 134515 (2003).
- [25] D. Hazra, L. M. A. Pascal, H. Courtois, and A. K. Gupta, Hysteresis in superconducting short weak links and μ -SQUIDs, Phys. Rev. B **82**, 184530 (2010).
- [26] F. Marsili, V. B. Verma, J. A. Stern, S. Harrington, A. E. Lita, T. Gerrits, I. Vayshenker, B. Baek, M. D. Shaw, R. P. Mirin, and S. W. Nam, Detecting single infrared photons with 93% system efficiency, Nat. Photonics **7**, 210 (2013).
- [27] K. K. Nagaev, Influence of electron-electron scattering on shot noise in diffusive contacts, Phys. Rev. B **52**, 4740 (1995).
- [28] D. Yu. Vodolazov and F. M. Peeters, Temporary cooling of quasiparticles and delay in voltage response of superconducting bridges after abruptly switching on the supercritical current, Phys. Rev. B **90**, 094504 (2014).
- [29] M.I. Kaganov, I.M. Lifshitz, and L.V. Talanov, Zh. Eksp. Teor. Fiz. **31**, 232 (1956).
- [30] N. Perrin and C. Vanneste, Response of superconducting films to a periodic optical irradiation, Phys. Rev. B **28**, 5150 (1983).
- [31] R.J. Watts-Tobin, Y. Krähenbühl, and L. Kramer, Nonequilibrium Theory of Dirty, Current-Carrying Superconductors: Phase-Slip Oscillators in Narrow Filaments Near T_c , J. Low Temp. Phys. **42**, 459 (1981).
- [32] A. Schmid, Kinetic equations for dirty superconductors (in book *Nonequilibrium Superconductivity, Phonons, and Kapitza Boundaries*, edited by K. E. Gray (Plenum Press, New York, 1981), p.423).
- [33] M. Caloz, B. Korzh, N. Timoney, M. Weiss, S. Gariglio, R. J. Warburton, Ch. Schonenberger, J. Renema, H. Zbinden, and F. Bussières, Optically probing the detection mechanism in a molybdenum silicide superconducting nanowire single-photon detector, arXiv:1611.08238.
- [34] D.Yu. Vodolazov, Yu.P. Korneeva, A.V. Semenov, A.A. Korneev, G.N. Goltsman, Vortex-assisted mechanism of photon counting in superconducting nanowire single photon detector revealed by external magnetic field, Phys. Rev. B **92**, 104503 (2015).
- [35] J.J. Renema, Q. Wang, R. Gaudio, I. Komen, K. op't Hoog, D. Sahin, A. Schilling, M. P. van Exter, A. Fiore, A. Engel, and J. A. de Dood, Position-dependent local detection efficiency in nanowire superconducting single-photon detector, Nano Lett. **15**, 4541 (2015).
- [36] D.Yu. Vodolazov, K. Ilin, M. Merker, M. Siegel, Defect-controlled vortex generation in current-carrying narrow superconducting strips, Supercond. Sci. Technol. **29**, 025002 (2016).
- [37] Yu. N. Ovchinnikov and V. Z. Kresin, Nonstationary state of superconductors: Application to nonequilibrium tunnelling detectors, Phys. Rev. B **58**, 12416 (1998).
- [38] A. G. Kozorezov, A. F. Volkov, J. K. Wigmore A. Peacock, A. Poelaert, and R. den Hartog, Quasiparticle-phonon downconversion in nonequilibrium superconductors, Phys. Rev. B **61**, 11807 (2000).
- [39] D. Yu. Vodolazov, Current dependence of the red boundary of superconducting single-photon detectors in the modified hot-spot model, Phys. Rev. B **90**, 054515 (2014).
- [40] W. J. Skocpol, M. R. Beasley, and M. Tinkham, Self-heating hotspots in superconducting thin-film microbridges, J. Appl. Phys. **45** 4054 (1974).
- [41] A.G. Kozorezov, C. Lambert, F. Marsili, M.J. Stevens,

- V.B. Verma, J.A. Stern, R. Horansky, S. Dyer, S. Duff, D.P. Pappas, A. Lita, M.D. Shaw, R.P. Mirin and S.W. Nam, Quasiparticle recombination in hotspots in superconducting current-carrying nanowires, *Phys. Rev. B* **92**, 064504 (2015).
- [42] F. Marsili, M. J. Stevens, A. Kozorezov, V. B. Verma, Colin Lambert, J. A. Stern, R. D. Horansky, S. Dyer, S. Duff, D. P. Pappas, A. E. Lita, M. D. Shaw, R. P. Mirin, and S. W. Nam, Hotspot relaxation dynamics in a current-carrying superconductor, *Phys. Rev. B* **93**, 094518 (2016).
- [43] J. J. Renema, R. Gaudio, Q. Wang, Z. Zhou, A. Gaggero, F. Mattioli, R. Leoni, D. Sahin, M. J. A. de Dood, A. Fiore, and M. P. van Exter, Experimental Test of Theories of the Detection Mechanism in a Nanowire Superconducting Single Photon Detector, *Phys. Rev. Lett.* **112**, 117604 (2014).
- [44] R. Lusche, A. Semenov, K. Ilin, M. Siegel, Y. Korneeva, A. Trifonov, A. Korneev, G. Goltsman, D. Vodolazov, H.-W. Hubers, Effect of the wire width on the intrinsic detection efficiency of superconducting nanowire single-photon detectors, *Journal of Applied Physics* **116**, 043906 (2014).
- [45] R. Gaudio, Z. Zhou, A. Fiore, J. J. Renema, M. P. van Exter, M.J.A. de Dood, V. B. Verma, A. E. Lita, J. Shainline, M. J. Stevens, R. P. Mirin, and S. W. Nam, Experimental investigation of the detection mechanism in WSi nanowire superconducting single photon detectors, *Appl. Phys. Lett.* **109**, 031101 (2016).
- [46] A. Engel, K. Inderbitzin, A. Schilling, R. Lusche, A. Semenov, H.-W. Hubers, D. Henrich, M. Hofherr, K. Ilin, and M. Siegel, Temperature-Dependence of Detection Efficiency in NbN and TaN SNSPD, *IEEE Trans. Appl. Supercond.* **23**, 2300505 (2013).